

DTIC FILE COPY

4

AD-A196 316

ARI-RR-644.1

AFGL-TR-88-0108

MOLECULAR LINE SHAPE EFFECTS ON ATMOSPHERIC
WINDOW ABSORPTION

J. Wormhoudt and R.C. Brown

Center for Chemical and Environmental Physics
Aerodyne Research, Inc.
45 Manning Road
Billerica, MA 01821

March 1988

Final Report
5 December 1985-4 March 1988

Approved for Public Release, Distribution Unlimited

AIR FORCE GEOPHYSICS LABORATORY
AIR FORCE SYSTEMS COMMAND
UNITED STATES AIR FORCE
HANSOM AFB, MA 01731-5000

DTIC
ELECTE
JUL 27 1988
S H D

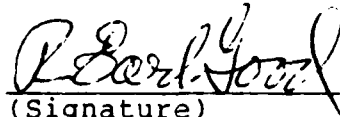
"This technical report has been reviewed and is approved for publication"

FOR THE COMMANDER



(Signature)

GEORGE A. VANASSE, Chief
Infrared Physics Branch



(Signature)

R. EARL GOOD, Acting Director
Optical Physics Division

This document has been reviewed by the ESD public Affairs Office (PA) and is releasable to the National Technical Information Service (NTIS).

Qualified requestors may obtain additional copies from the Defense Technical Information Center. All others should apply to the National Technical Information Service.

If your address has changed, or if you wish to be removed from the mailing list, or if the addressee is no longer employed by your organization, please notify AFGL/DAA, Hanscom AFB, MA 01731. This will assist us in maintaining a current mailing list.

Do not return copies of this report unless contractual obligations or notices on a specific document requires that it be returned.

Unclassified

SECURITY CLASSIFICATION OF THIS PAGE

REPORT DOCUMENTATION PAGE

1a. REPORT SECURITY CLASSIFICATION Unclassified			1b. RESTRICTIVE MARKINGS	
2a. SECURITY CLASSIFICATION AUTHORITY			3. DISTRIBUTION/AVAILABILITY OF REPORT Approved for public release; distribution unlimited	
3b. DECLASSIFICATION/DOWNGRADING SCHEDULE				
4. PERFORMING ORGANIZATION REPORT NUMBER(S) ARI-RR-644.1			5. MONITORING ORGANIZATION REPORT NUMBER(S) AFGL-TR-88-0108	
5a. NAME OF PERFORMING ORGANIZATION Aerodyne Research, Inc.		6b. OFFICE SYMBOL (If applicable)		7a. NAME OF MONITORING ORGANIZATION Air Force Geophysics Laboratory
5c. ADDRESS (City, State, and ZIP Code) 45 Manning Road Billerica, MA 01821-3976			7b. ADDRESS (City, State, and ZIP Code) Hanscom Air Force Base Bedford, Massachusetts 01731	
8a. NAME OF FUNDING/SPONSORING ORGANIZATION		8b. OFFICE SYMBOL (If applicable)		9. PROCUREMENT INSTRUMENT IDENTIFICATION NUMBER F19628-85-C-0183
8c. ADDRESS (City, State, and ZIP Code)			10. SOURCE OF FUNDING NUMBERS	
			PROGRAM ELEMENT NO. 61102F	PROJECT NO. 2310
			TASK NO. G1	WORK UNIT ACCESSION NO. B1
11. TITLE (Include Security Classification) Molecular Line Shape Effects on Atmospheric Window Absorption				
12. PERSONAL AUTHOR(S) J. Wormhoudt, R.C. Brown				
13a. TYPE OF REPORT FINAL REPORT		13b. TIME COVERED FROM 12/05/85 TO 3/04/88		14. DATE OF REPORT (Year, Month, Day) 1988 March
15. PAGE COUNT 70				
16. SUPPLEMENTARY NOTATION				
17. COSATI CODES			18. SUBJECT TERMS (Continue on reverse if necessary and identify by block number)	
FIELD	GROUP	SUB-GROUP		
			Atmospheric Absorption; continuum absorption; atmospheric windows	
19. ABSTRACT (Continue on reverse if necessary and identify by block number)				
<p>Two theoretical approaches have been followed to calculate far wing absorption of collision reduced absorption in the infrared. The first approach was a standard time dependent perturbation theory. Two methods of this kind were pursued, using different limits. A second approach was investigated called the Recursive Residue Generation Method. The first approach was applied to water self-broadening. Results are given in 10 μm region. The second approach was investigated for feasibility and examined in the context of the HCl-Ar wings.</p>				
20. DISTRIBUTION/AVAILABILITY OF ABSTRACT <input type="checkbox"/> UNCLASSIFIED/UNLIMITED <input type="checkbox"/> SAME AS RPT. <input type="checkbox"/> DTIC USERS			21. ABSTRACT SECURITY CLASSIFICATION Unclassified	
22a. NAME OF RESPONSIBLE INDIVIDUAL Laurence S. Rothman			22b. TELEPHONE (Include Area Code)	22c. OFFICE SYMBOL AFGL/OPI

TABLE OF CONTENTS

<u>Section</u>	<u>Page</u>
1 INTRODUCTION	1-1
1.1 Background and Research Objectives	1-2
1.2 Report Outline	1-5
2 OVERVIEW OF THEORETICAL METHODS	2-1
2.1 Autocorrelation Function Formulation of the Line Shape	2-1
2.2 Uncoupled Lines and Binary Collision Approximations ...	2-2
3 APPLICATION OF DTC THEORY TO H ₂ O SELF-BROADENING	3-1
3.1 H ₂ O Absorption In the 10 μ m Region	3-1
3.2 Application to H ₂ O Self-Broadening	3-3
3.3 Temperature Dependence of the Halfwidth Function in DTC Theory	3-5
4 CUT-OFF FREE THEORY FOR ROTATIONAL LINESHAPES	4-1
4.1 Generalized Leavitt-Korff Theory of Line Broadening	4-1
4.2 Comparison with Davies, Tipping, and Clough for H ₂ O Self-Broadening	4-5
5 RECURSIVE RESIDUE GENERATION METHOD	5-1
5.1 General Description of the Method	5-1
5.2 Application to HCl-Ar	5-4
5.2.1 System Hamiltonian and Matrix Elements	5-4
5.2.2 Dipole Autocorrelation Function	5-7
5.2.3 Preliminary Results	5-10
6 SUMMARY	6-1
7 REFERENCES	7-1

APPENDIX A DERIVATION OF DAVIES, TIPPING, AND CLOUGH LINESHAPE FUNCTION

APPENDIX B COUPLING MATRIX ELEMENTS OF THE LONG RANGE ANISOTROPIC INTERACTION

APPENDIX C RADIAL MATRIX ELEMENTS OF $R^{-\lambda}$



Distribution For	
GRA&I	<input checked="" type="checkbox"/>
TAB	<input type="checkbox"/>
Unannounced	<input type="checkbox"/>
Justification	
By	
Distribution/	
Availability Codes	
Dist	Avail and/or Special
A-1	

1. INTRODUCTION

Long path atmospheric transmission in atmospheric window bands such as the 3-5 μm , 8-12 μm , and millimeter wave regions can be limited by absorption in the line wings. There are now a number of critical military applications, including infrared search and track detection of cruise missiles and bombers, infrared imaging from space, millimeter wave communications, laser target designation, and laser weapons beam propagation which require detailed knowledge of absorption lineshapes and their influence on atmospheric radiation transport. There are also potential geophysical applications such as atmospheric sounding and trace species monitoring which require better lineshape knowledge than that currently available. Lastly, there is still active interest in energy fluxes in planetary atmospheres and the global radiation budget, which motivated the first studies of atmospheric window transmission.

These needs have resulted in the development of a large body of atmospheric transmission calculation technology, primarily through the Air Force Geophysics Laboratory (AFGL). Development continues on sophisticated computer codes such as the AFGL LOWTRAN family for low spectral resolution and FASCODE, based on the AFGL line parameters compilation. For both codes, the largest uncertainties are in continuum components which dominate in window bands.¹ This has generated continued interest, including diode laser and conventional absorption spectroscopy experiments, AFGL workshops on high resolution atmospheric transmission and yearly AFGL Symposia on Seeing Through the Atmosphere, as well as an International Workshop on Atmospheric Water Vapor.²

This is the tenth and final R&D Status Report for Contract Number F19628-85-C-0183, "Molecular Line Shape Effects on Atmospheric Window Absorption". It covers work through contract termination on February 3, 1988, and includes a review of all work on the contract since the start date of September 9, 1985. The objective of the program was to develop theoretical methods for predicting the shape of molecular absorption lines in the wing regions. The investigation included but was not limited to asymptotically correct forms valid in the far wings and near line center (to give line widths). Its motivation was to assess the effect of line shapes on atmospheric window absorption, so that systems of particular interest included water-water, water-nitrogen, and carbon dioxide-nitrogen. Particular emphasis was placed on the temperature dependence of line shapes and widths, since these are among the most sensitive experimental tests of detailed theories.

1.1 Background and Research Objectives

The shape of infrared spectral line near line center is known to be well described by the Lorentz function. The problem of calculating absorption near the center of a strong line is therefore that of computation of the Lorentz width. Microscopic theoretical formulations are available which allow evaluation of a width operator in terms of intermolecular potentials. From the assumptions used in deriving easily evaluated expressions for the width operator which are valid near line center, (or simply from the requirement that the integrated absorption over the entire lineshape must be finite), it is clear that at some point in the line wing, the Lorentz function can no longer be correct. The problem of predicting the wing functional form as well as absolute magnitude has attracted much attention, but work to date has produced either formal derivations which stop short of numerical results, or calculations of wing behavior which are highly approximate.

Davies, Tipping and Clough^{3,4} (DTC) developed an explicitly time dependent theory for spectral line broadening based on the dipole moment autocorrelation function. In contrast to earlier treatments, the DTC theory is fully quantum mechanical and rigorously satisfies the fluctuation dissipation theorem on a microscopic level. In addition, whereas alternate quantum mechanical approaches^{5,6} (e.g. those based on close-coupling calculations or various approximations thereof) are typically limited to line widths for smaller molecular systems, the DTC formulation provides the entire frequency dependent absorption profile for more complicated molecular systems.

The DTC formulation relies on two basic approximations. First, it is assumed that the many body collisional problem for far wing absorption can be, at least qualitatively, reduced to treatment of the scattering interaction between a single pair of absorbing (radiator) and perturbing molecules and then simply multiplying by the total number of such pairs. Second, it is assumed that the anisotropic intermolecular interaction is sufficiently weak to permit the time dependent scattering transition probabilities to be treated using perturbation theory. Although there is some evidence that the so-called single-perturber approximation does qualitatively reproduce observed spectral features at low gas densities,^{7,8} the reliance on perturbation theory is more problematic.

One unresolved issue associated with perturbative treatments of line broadening is the implicit restrictions on the intermolecular interactions which may contribute to far-wing absorption. For example, scattering resonances and/or complex formation cannot be adequately treated within the DTC formulation; rather, it is generally assumed that the dominant interactions responsible for far-wing absorption arise from long range anisotropic interactions. However, even in this case, perturbation theory breaks down as the impact parameter approaches zero. Practical applications,

therefore, require ad-hoc cutoff functions which ensure physically reasonable values for the absorption coefficient in strong collision regimes.

Davies and Fahey used the DTC theory, assuming dipole-dipole and dipole-quadrupole interactions and neglecting line coupling effects, to treat far-wing continuum absorption for the $\text{H}_2\text{O}-\text{H}_2\text{O}$ system.⁴ We have also used DTC theory to study this system. In both cases it was found that the calculated profile failed to agree with available experimental data. In particular, the theoretical far-wing absorption cross sections had the wrong temperature dependence. In addition, our analysis indicated that the cutoff functions needed to ensure well behaved absorption profiles under strong intermolecular interactions were affecting the $\text{H}_2\text{O}-\text{H}_2\text{O}$ line shapes out to 1000 cm^{-1} off line center.

On the basis of this analysis it was suggested that additional research was needed to develop theoretical methods which were either nonperturbative or, at least, less dependent upon ad hoc cutoff functions to deal with strong collisions between the radiating and perturbing species. In addition, it was also suggested that the theoretical methods and corresponding computer codes should be more general with respect to the type of intermolecular interactions with which they can deal.

Accordingly, our research has focused on developing two theoretical methods which showed promise for achieving these goals. Both methods are based on the dipole autocorrelation function formulation and assume uncoupled lines and the binary collision approximation. The first method, discussed in Section 4, is based on a generalization of the Leavitt-Korff cutoff-free impact theory of line broadening.⁹ This method, although based on perturbation theory, uses a linked-cluster resummation of the perturbation expansion to yield absorption cross sections which remain well-behaved in strong collision regimes without resorting to ad hoc cutoff functions. The

second technique, the Recursive-Residue-Generation Method (RRGM)^{10,11} is a nonperturbative method which can treat arbitrary intermolecular interactions.

1.2 Report Outline

Section 2 discusses the basic approach and common approximations invoked by the theoretical methods described in this report. Section 3 describes the application of the DTC method (developed in Appendix A) to H₂O self-broadening. Section 4 describes the GLK method and gives results for the H₂O self-broadening. Section 5 describes the RRGGM method which is illustrated by an application to HCl-Ar. A summary is presented in Section 6.

Some mathematical details are treated in the Appendices. In addition to a formal description of the DTC lineshape in Appendix A, Appendix B and C contain a description of the matrix elements of high order multipole interaction and computational techniques for radial matrix elements, respectively.

2.0 OVERVIEW OF THEORETICAL METHODS

2.1 Autocorrelation Function Formulation of the Line Shape

The absorption coefficient per unit path length, $\alpha(\omega)$, for a dilute gas is related to the thermally averaged dipole autocorrelation function for the system, $\Phi(t)$, by¹²

$$\alpha(\omega) = \frac{4\pi\omega n_r^2}{3c} (1 - e^{-\beta\hbar\omega}) \int_{-\infty}^{\infty} \frac{dt}{2\pi\hbar} e^{-i\omega t} \Phi(t) \quad (2-1)$$

where $\beta = 1/k_B T$, n_r is the number density of radiating dipoles, and $\Phi(t)$ is the dipole autocorrelation function for a single radiator interacting with N_p perturbers,

$$\Phi(t) = \text{Tr}[\rho(0) \vec{\mu} \cdot \{e^{iHt/\hbar} \vec{\mu} e^{-iHt/\hbar}\}] \quad (2-2)$$

where $\rho(0)$ is the initial density matrix, $\vec{\mu}$ is the initial dipole moment operator and H is the Hamiltonian operator for the system. We shall assume a canonical system so that

$$\rho(0) = \rho(H) = \frac{e^{-\beta H}}{\text{Tr}(e^{-\beta H})} = \frac{e^{-\beta H}}{Q_p} \quad (2-3)$$

is the canonical density operator with partition function Q_p . In addition, the present report will specifically treat foreign broadening by perturbing molecules which do not absorb in the spectral regions of interest. The dipole moment operator is then $\vec{\mu} = \vec{\mu}_r$ where $\vec{\mu}_r$ is the dipole moment of the absorbing species (radiator). However, self-broadening may be treated in basically the

same fashion.⁴ Lastly, defining the complex time variable $z = t - i\beta\hbar$ and using the cyclic invariance of the trace operation, Eq. (2.2) can be rewritten as

$$\phi(t) = \frac{1}{Q_p} \text{Tr}[\vec{\mu} \cdot \{ e^{iHt/\hbar} \vec{\mu} e^{-iHz/\hbar} \}] \quad (2-4)$$

where the Boltzmann statistical weight has been incorporated into the time evolution of the dipole moment operator.

2.2 Uncoupled lines and Binary Collision Approximations

All calculations in this report will assume uncoupled lines and the binary collision approximation. The uncoupled line approximation assumes that there are not collision induced correlations between zero-order transitions. Then, the autocorrelation function may be expressed as a sum of correlation functions for each dipole transition, i.e.,

$$\phi(t) = \sum_i \sum_f \phi_{if}(t)$$

where i and f refer to initial and final states. The binary collision approximation assumes that the N_p perturber autocorrelation function is simply the product of N_p identical single-perturber autocorrelation functions. In this case it is shown in Appendix A that

$$\phi_{if}(t) \propto e^{i\omega_{if}T} e^{-n_p \Omega \Psi_{if}(t)}$$

where ω_{if} is the transition frequency, n_p the perturber intensity, Ω the system volume, and Ψ_{if} is approximately a properly normalized single perturber correlation function.

3.0 APPLICATION OF DTC THEORY TO H₂O SELF-BROADENING

3.1 H₂O Absorption In the 10 μ m Region

For atmospheric "window" transmission, H₂O absorption is particularly important in the 10 μ m region. It is generally thought that absorption in this region is due to wings of lines in the 6.3 μ m and pure rotation bands. It has also been speculated that dimers (H₂O • H₂O or H₂O • N₂) or larger clusters may be responsible for much of the absorption. Since line wing and dimer absorption have the same pressure dependence, and indeed, at observed temperatures could have the same continuum spectral appearance, it is not possible to distinguish between different mechanisms from present experimental or theoretical work.

Line wing absorption is often reported as the ratio of observed absorption to that expected for a Lorentzian lineshape. This ratio is denoted χ . At this time, the general observation is that water continuum absorption in the extreme wings lies below the absorption predicted by summing the Lorentzian line wings from pure rotational transitions.¹³ This is illustrated in Figure 3.1 which displays the temperature dependent χ factor corresponding to the ratio of the experimental absorption to the absorption computed by summing Lorentzians for all distant lines on the HITRAN tape, after subtracting out all nearby lines.^{14,15}

In Figure 3.1, the experimental χ factors at 1000 cm⁻¹ range from 0.1 to 0.6 and decrease with increasing temperature. To understand the theoretically predicted temperature dependence of far wing absorption, the DTC formulation was used to treat a few isolated H₂O rotational lines. The model system and results are presented in Section 3.2. The predicted temperature dependence is discussed in Section 3.3.

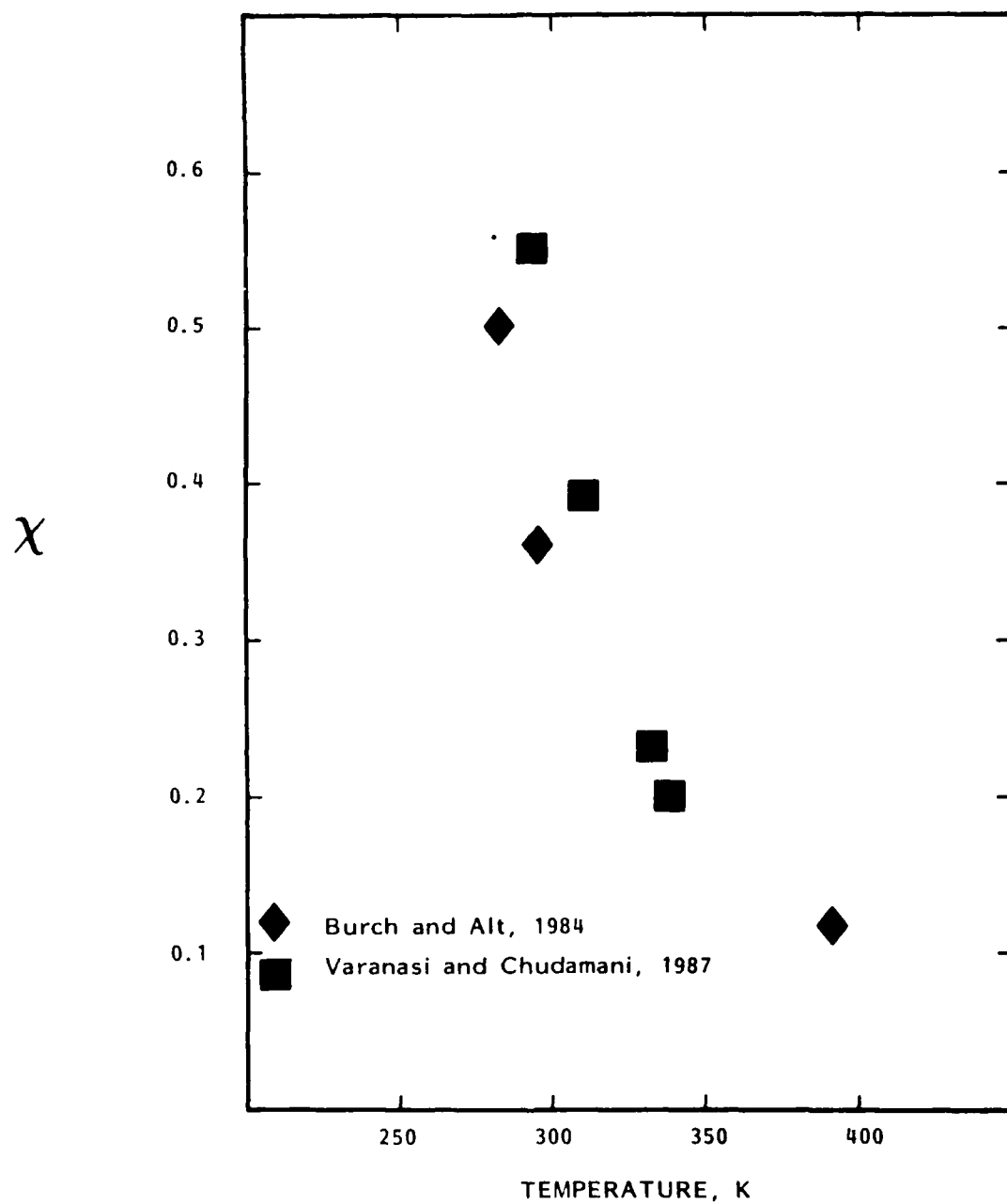


Figure 3.1. Experimental Water Continuum As Lorentzian Correction, χ , at 1000 cm^{-1}

3.2 Application to H₂O Self-Broadening

The DTC method, assuming uncoupled lines and the binary collision approximation, was used to treat a few isolated lines for the H₂O/H₂O system. The zeroth-order Hamiltonian is given by

$$H_o = H_R^o + H_P^o + H_{RP}^o$$

where H_R^o , H_P^o are rigid rotor Hamiltonians for the H₂O molecules with

eigenstates $|j, \tau, m\rangle$ and eigenvalues $\xi(j, \tau)$. The operator H_{RP}^o describing the

relative motion of the H₂O molecules is given by

$$H_{RP}^o = \frac{\hbar^2}{2\mu R^2} \frac{\partial}{\partial R} R^2 \frac{\partial}{\partial R} + \frac{L^2}{2\mu R^2}$$

where μ is the reduced mass for two point particles with reduced mass $\mu = H_2O$

R is the intermolecular separation, and L is the total angular momentum.

Using the spherical harmonics satisfying

$$L^2 | \ell m \rangle = \hbar^2 \ell(\ell + 1) | \ell m \rangle$$

$$L | \ell m \rangle = \hbar m | \ell m \rangle$$

the stationary states of H_{RP}^0 can be expressed as $|\ell\mu\xi\rangle =$

$|\ell\mu\rangle |\ell\xi\rangle$ where the radial eigenfunctions satisfy

$$\left[-\frac{\hbar^2}{2\mu R^2} \frac{\partial}{\partial R} + \frac{\hbar^2 \ell(\ell+1)}{2\mu R^2} + V_0(R) \right] |\ell\xi\rangle = E_\ell |\ell\xi\rangle$$

For the present calculation the isotopic intermolecular interaction has been modeled by a 6-12 Lennard-Jones potential

$$V_0(R) = V_0 \left[\left(\frac{6}{R} \right)^{12} - 2 \left(\frac{6}{R} \right)^6 \right]$$

The anisotropic coupling interaction responsible for modifying the H_2O rotational lines was represented as an multiple expansion which includes terms through electrostatic dipole/quadrupole.

$$V(R, \theta, \phi) = V_{DD}(R, \theta, \phi) + V_{DQ}(R, \theta, \phi) + V_{QD}(R, \theta, \phi)$$

In a cartesian coordinate system these terms are given by

$$V_{DD} = \frac{1}{R^3} [\vec{\mu}_1 \cdot \vec{\mu}_2 - 3(\vec{\mu}_1 \cdot \vec{R})(\vec{\mu}_2 \cdot \vec{R})]$$

$$V_{DQ} = \frac{3}{2R^4} [2\vec{R} \cdot \vec{Q}_2 \cdot \vec{\mu}_1 - 5(\vec{R} \cdot \vec{\mu}_1)(\vec{R} \cdot \vec{Q}_2 \cdot \vec{R})]$$

where μ_1 , μ_2 and Q_1 and Q_2 are dipole and quadrupole cartesian tensors for the radiator (1) and perturber (2), respectively. Parameter values are given in Reference 4.

The DTC chi-factors at 1000 cm^{-1} for the $(4,1,5) \rightarrow (5,2,5)$ H_2O rotational transition are shown in Figure 3.2. In addition to being an order of magnitude smaller than the experimental results the theoretical chi-factors

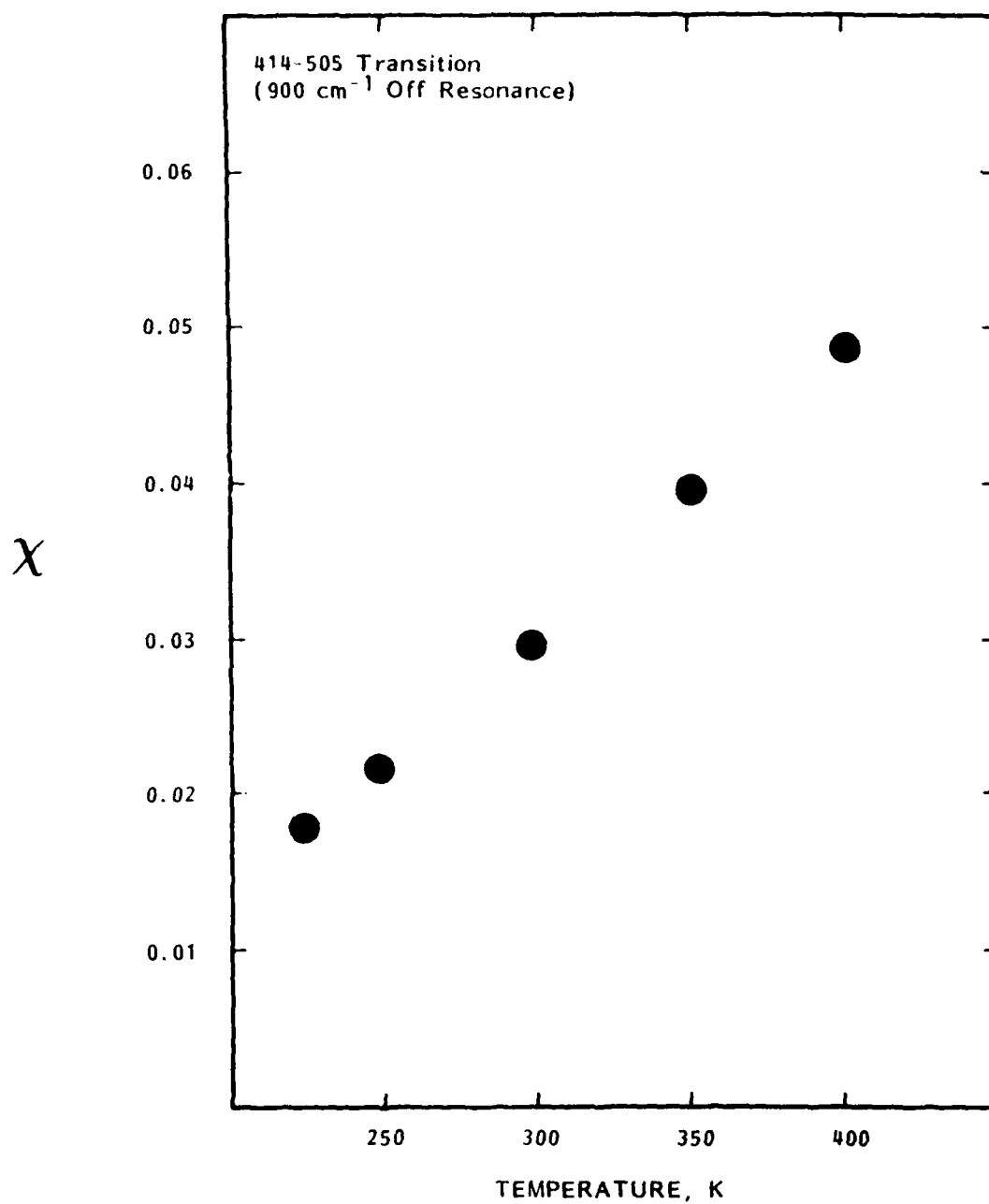


Figure 3.2. Calculated Water Line Wing Absorption As Lorentzian Correction, χ , At 1000 cm^{-1}

also show a positive temperature dependence. We were able to show that this is not unexpected, using simple qualitative arguments. We review that work here.

3.3 Temperature Dependence of the Halfwidth Function in DTC Theory

Simple models to correlate DTC results can be found in analytic approximations to Anderson theory for line widths. A particularly useful review is given by Birnbaum in Volume 12 of *Advances in Chemical Physics*. It is shown that the line broadening cross section consists of two factors. The first is a coefficient which is proportional to a power of the temperature. The second is a function of a resonance factor which is proportional to the total change in rotational energy of the absorbing and colliding molecules.

Much rule-of thumb analysis of linewidth temperature behavior is done by assuming that in the important line broadening collisions, total changes in rotational energy and therefore the resonance factor are small, and its function remains near one. In that case, the power of the temperature corresponding to the DTC definition of the linewidth is $(n-3)/(n-1)$, where n is the exponent varies from zero to one-half as the potential is varied from dipole-dipole ($n=3$) to hard-sphere. The DTC predictions on resonance lie within this range, but for non-resonant photons the predictions increase much more rapidly with increasing temperature.

In fact there is no reason for the water-water system to follow the above simple dependence. For non-resonant photons, the resonance factor (which is essentially the collisional change in momentum required to conserve energy) contains the difference between the photon and transition energies. Large contributions are obtained with transitions with small resonance factors, except that each transition is weighted by the Boltzmann factor for the initial rotational state of the perturber. That weighting determines an average, non-zero resonance factor.

By taking the resonance factor function to be an exponential of a power of the inverse temperature, one can deduce averages of the translational energy change during a collision by fitting the resulting exponential expression to the predicted DTC temperature dependence for the (4,1,4) - (5,0,5) transition. The variation in this quantity with varying photon energy, with excluding or including dipole-quadrupole forces, and between the initial- and final-state contributions is with only one exception in accordance with the expectation that larger average translational energy changes will be associated with smaller, more-temperature dependent terms. The one possible discrepancy, between the two potential choices for the initial state term and a 1000 cm^{-1} photon, may be due to the different weighting of perturber rotational transitions in the two cases.

In order to investigate the details of which collisional transitions are most important, we developed a computer program (S2TERM) which read the same input files as the DTC HWIDTH program, for a single translational energy and angular momentum quantum number (ℓ). S2TERM examines the contributions to the linewidth function from all rotational transitions in absorber and perturber, then prints out data for only those whose contribution is above a certain fraction of the total. The simplification is impressive - for example, for the (11,3,8) - (12,4,9) dipole-quadrupole and quadrupole-dipole calculations for $\ell = 0$, 400 cm^{-1} translational energy and a 1211.3 cm^{-1} photon energy, 47 and 59 terms out of 10,000 give over half and almost two-thirds of the totals.

The data printed out in the S2TERM lists include the changes in absorber and perturber rotational energy and relative translational energy, the Boltzmann factor for the perturber initial rotational state, the transition strengths for both rotational changes, and the matrix element appropriate to the residual change in translational energy. It is the product of the last four terms that determines the contribution from a given pair of rotational transitions.

The sum of the three collisional energy changes satisfy an energy conservation relation with the difference between the photon and transition energies. The relation is different for the initial and final state terms. Using the notation in the GTE final report is

$$(\varepsilon_{j_i} - \varepsilon_{j'_i}) + (\varepsilon_J - \varepsilon_{J'}) + (\varepsilon_k - \varepsilon_{k'}) - (\omega - \omega_{fi}) = 0$$

for the initial state term, and

$$(\varepsilon_{j_f} - \varepsilon_{j'_f}) + (\varepsilon_J - \varepsilon_{J'}) + (\varepsilon_k - \varepsilon_{k'}) + (\omega - \omega_{fi}) = 0$$

for the final state. If we designate the first three terms as $\Delta\varepsilon_{\text{coll}}$, these relationships can be illustrated as follows,

$$\begin{array}{ccc} j_f J k \text{---} & & j_f' J k' \text{---} \\ j_i J k \text{---} \omega_{fi} & & \Delta\varepsilon_{\text{coll}} \quad \omega \\ \Delta\varepsilon_{\text{coll}} \quad \omega & & j_f J k \text{---} \omega_{fi} \\ j'_i J' k' \text{---} & & j_i J k \text{---} \end{array}$$

It can be seen that for initial absorber states of relatively low energy, much of the downward change in system energy required to accommodate the off-resonance photon will have to come either from perturber transitions from high rotational states with small Boltzmann weightings, or from large changes in translational energy giving rise to small matrix elements. There are no such constraints on the final state term, so that in the far (blue) wing the important terms in its sum are one to two orders of magnitude larger than those contributing to the initial state cross section. However, the energy needed to carry the state f into f' should also appear in a Boltzmann weighting, and the inverse of the factor $e[-\beta\hbar(\omega-\omega_{fi})]$ (a detailed balance factor) multiplying the initial state term restores the proper ratio.

In the low-J (strong line) cases studied, the final and detailed balance weighted initial state terms are of the same order of magnitude. Although the detailed balance factor has a very strong negative temperature dependence, much like that actually observed in water-water far wing absorption, the initial state term for low J's has a very strong positive temperature dependence as well as a small magnitude (both due to perturber rotational Boltzmann factors). Meanwhile, the contributions from the final state term come mostly from higher J transitions as well, since high transition strengths and large translational matrix elements (when a transition between two high J's can make up most of the energy difference) make up for smaller perturber rotational populations. The result of these trends is the strong positive temperature dependence seen in the GTE predictions.

This temperature dependence is less strong when dipole-quadrupole forces are included. It is reasonable to expect some further improvement is quadrupole-quadrupole forces were included. It is also less strong for absorbers in high initial rotational states. S2TERM analysis shows these trends to be explained by the above discussion, specifically by changes in the perturber J states which can contribute and the resulting changes in cross section magnitude and temperature dependence. We ran GTE far wing predictions for two high-J and two low-J transitions, and found no behavior which could not be correlated as described above. Although high-J lines have negative temperature dependence and super-Lorentzian wings as do the observed wings, their intensities are much too small for them to make significant contributions.

One conclusion which can be drawn from the above investigations and our earlier work on the unimportance of bound and quasi-bound states is that the only source of strong negative temperature dependence of wing absorption is the detailed balance factor. If this were true, one would expect that the observed temperature dependence would become more strongly negative with increasing frequency difference from line center. Our analysis of the data

reported by Burch seems indeed to show a variation in the temperature exponent that parallels that obtained from fitting the exponential in inverse temperature to a T^{-n} form.

The observations are not so precise that any agreement would constitute proof, and in fact the observed exponent seems to be about one higher than that obtained from the detailed balance term alone, without any modifications by linewidth factors which still will increase with temperature. On the other hand, comparison with experiment does not seem to rule out the possibility that a predictive method based on the GTE model, but with additional transitions included to improve linewidth term magnitudes and temperature dependences, might in fact be an accurate description of wing absorption.

4.0 CUT-OFF FREE THEORY FOR ROTATIONAL LINESHAPES

4.1 Generalized Leavitt-Korff Theory of Line Broadening

Leavitt and Korff⁹ derived a variation on Anderson's impact theory¹⁶ of line broadening which remains well-behaved as the impact parameter approaches zero. Consequently, applications do not require ad hoc cutoff functions to preserve unitarity in strong collision regimes. There are two key features to their derivation. First, it is assumed that the time evolution operator is both energy conserving and invariant with respect to orientations of the radiating and perturbing molecules. Second, a linked-cluster theorem for degenerate states is used to decompose each order in the perturbation series in terms of its linked-cluster expansion. Subsequent factorization and resummation then yields an expression for the interruption function in which Anderson's S_2 -functions¹⁶ have been exponentiated. In this section, the Leavitt-Korff half-width theory is generalized for frequency dependent lineshapes.

In Equation (A.14), the Hamiltonian \tilde{H}_0 (for convenience we will drop the superscript and subscript s notation) for a single perturber interacting with the radiating molecule is

$$\tilde{H}_0 = H_P^0 + H_{RP}^0 \quad (4-1)$$

where H_P^0 is the rigid rotor Hamiltonian for the perturber with eigenstates

$$H_P^0 | \lambda_P \rangle = H_P^0 | j_P \tau_P m_P \rangle = E_{j_P \tau_P} | j_P \tau_P m_P \rangle \quad (4-2)$$

is the Hamiltonian operator for two structureless particles interacting through a two-body local isotropic potential $V^0(R)$

$$H_{RP}^0 = [-\frac{\hbar^2}{2u} \vec{\nabla}^2 + V^0(R)] \quad (4-3)$$

The stationary states of H_{RP}^0 are

$$H_{RP}^0 | \vec{k} \rangle = H_{RP}^0 | \ell m_\ell \varepsilon \rangle \quad (4-4)$$

Using these zeroth-order states, the trace in Equation (A-14) can be evaluated to give

$$\begin{aligned} \tilde{\text{Tr}}[\dots] = \sum_{\lambda_p} \sum_{\vec{k}} \sum_{\lambda'_p} \sum_{\vec{k}'} \rho(E_{j_p \tau_p} + \varepsilon) \langle j_i \tau_i m'_i \lambda_p \vec{k} | U(z) | j_i \tau_i m_i \lambda'_p \vec{k}' \rangle \\ \times \langle j_f \tau_f m_f \lambda'_p \vec{k}' | U^+(t) | j_f \tau_f m'_f \lambda_p \vec{k} \rangle \end{aligned} \quad (4-5)$$

As a first approximation to Equation (4.6a) it is assumed that the matrix elements of the time evolution operators are approximately given by

$$\langle j_i \tau_i m'_i \lambda_p \vec{k} | U(z) | j_i \tau_i m_i \lambda'_p \vec{k}' \rangle \approx \delta_{m_i m'_i} \delta_{\lambda_p \lambda'_p} \delta_{\vec{k}, \vec{k}'} \bar{U}_i(z) \quad (4-6a)$$

$$\langle j_f \tau_f m'_f \lambda'_p \vec{k}' | U^+(z) | j_f \tau_f m_f \lambda_p \vec{k} \rangle \approx \delta_{m_f m'_f} \delta_{\lambda_p \lambda'_p} \delta_{\vec{k}, \vec{k}'} \bar{U}_f^+(t) \quad (4-6b)$$

where

$$\bar{U}_i(z) = [(2j_i+1)(2j_p+1)(2\ell+1)]^{-1} \sum_{m_i} \sum_{m_p} \sum_{m_\ell} \langle j_i \tau_i m_i \lambda_p \vec{k} | U(z) | j_i \tau_i m_i \lambda_p \vec{k} \rangle \quad (4-7a)$$

and

$$\bar{U}_f^+(z) = [(2j_f+1)(2j_p+1)(2\ell+1)]^{-1} \sum_{m_f} \sum_{m_p} \sum_{m_\ell} \langle j_f \tau_f m_f \lambda_p \vec{k} | U^\dagger(t) | j_f \tau_f m_f \lambda_p \vec{k} \rangle \quad (4-7b)$$

As in Reference (1), the basis of this approximation is that the resulting expression for autocorrelation function reduces to that given by DTC when the perturbation is weak. Substituting Equation (4-6) into Equation (4-5) gives

$$\tilde{\text{Tr}}[\dots] = \delta_{m_i m_i'} \delta_{m_f m_f'} \sum_{j_p} \sum_{\tau_p} \sum_{\ell} \int d\varepsilon (2j_p+1)(2\ell+1) \rho(E_{j_p \tau_p} + \varepsilon) \bar{U}_i(z) \bar{U}_f^+(t)$$

Then, substituting Equation (4-8) back into Equation (A-14) and performing the summations of magnetic quantum numbers gives

$$Q_{if}(t) = \sum_{j_p} \sum_{\tau_p} \sum_{\ell} \int d\varepsilon (2j_p+1)(2\ell+1) \rho(E_{j_p \tau_p} + \varepsilon) \bar{U}_i(z) \bar{U}_f^+(t) \quad (4-9)$$

The matrix elements \bar{U}_i and \bar{U}_f can be evaluated using the linked-cluster theorem for degenerate states as described in Reference (9) giving

$$\bar{U}_i(z) = e^{\sum_n S_{n,i}(z)} \quad (4-10a)$$

$$\bar{U}_f^+(t) = e^{\sum_n S_{n,f}(t)} \quad (4-10b)$$

where the S_n functions are

$$S_{n,i}(z) = (-i/\hbar)^n \int_0^z dz_1 \dots \int_0^{z_{n-1}} dz_n [(2j_i+1)(2j_p+1)(2\ell+1)]^{-1}$$

$$\times \sum_{m_i} \sum_{m_p} \sum_{m_\ell} \langle \lambda_i \lambda_p \vec{k} \mid [V(z_1) \dots V(z_n)]_L^{(0)} \mid \lambda_i \lambda_p \vec{k} \rangle \quad (4-11a)$$

and

$$S_{n,f}(t) = (-i/\hbar)^n \int_0^t dt_1 \dots \int_0^{t_{n-1}} dt_n [(2j_f+1)(2j_p+1)(2\ell+1)]^{-1} \\ \times \sum_{m_f} \sum_{m_p} \sum_{m_\ell} \langle \lambda_f \lambda_p \vec{k} \mid [V(t_1) \dots V(t_n)]_L^{(0)} \mid \lambda_f \lambda_p \vec{k} \rangle \quad (4-11b)$$

As in Reference (9), the subscript L indicates that in evaluating the quantity in brackets all subproducts which are diagonal in all quantum numbers and rotationally invariant in the spaces of the radiator, perturber and radial vector \vec{R} are excluded, while the superscript (0) indicates that the entire quantity is rotationally invariant. As noted in Reference (9), the first order terms $S_{1,i}$ and $S_{1,f}$ are complex and only contribute to the line shift. The S_2 -functions are then the first terms to contribute to line broadening. These are given by

$$S_{2,i}(z) = -(1/\hbar)^2 \int_0^z dz_1 \int_0^{z_1} dz_2 [(2j_i+1)(2j_p+1)(2\ell+1)]^{-1} \times \sum_{\lambda'_i} \sum_{\lambda'_p} \sum_{\vec{k}'} \\ \times \sum_{m_i} \sum_{m_p} \sum_{m_\ell} \langle \lambda_i \lambda_p \vec{k} \mid V(z_1) \mid \lambda'_i \lambda'_p \vec{k}' \rangle \langle \lambda'_i \lambda'_p \vec{k}' \mid V(z_2) \mid \lambda_i \lambda_p \vec{k} \rangle \quad (4-12a)$$

$$S_{2,f}(t) = -(1/\hbar)^2 \int_0^t dt_1 \int_0^{t_1} dt_2 [(2j_f+1)(2j_p+1)(2\ell+1)]^{-1} \times \sum_{\lambda'_f} \sum_{\lambda'_p} \sum_{\vec{k}'}$$

$$\times \sum_{m_i} \sum_{m_p} \sum_{m_\ell} \langle \lambda_i \lambda_p \vec{k} | V(t_1) | \lambda'_i \lambda'_p \vec{k}' \rangle \langle \lambda'_i \lambda'_p \vec{k}' | V(t_2) | \lambda_i \lambda_p \vec{k} \rangle \quad (4-12b)$$

where the primes on the summations indicate that no diagonal terms are to be included in the summation. Then, up through second order in the interaction, the single-perturber autocorrelation function is

$$Q_{if}(\tau) = \sum_{j_p} \sum_{\tau_p} \sum_{\ell} \int d\varepsilon \rho(E_{j_p \tau_p} + \varepsilon) e^{S_{2,i}(z) + S_{2,f}(t)} \quad (4-13)$$

Details for evaluating matrix elements of the anisotropic interaction potential V , assuming a multipole expansion are given in Appendices B and C, for arbitrary orders of the multipolar tensors.

4.2 Comparison With Davies, Tipping and Clough for H₂O Self-Broadening

The generalized-Leaviff-Korff approach was used to treat H₂O self-broadening using the molecular Hamiltonian given in Section 3.2. Figure 4.1 shows chi-factors obtained from the DTC and GLK methods out to 900 cm⁻¹ off line center, assuming dipole-dipole interactions only. At 100 cm⁻¹ the DTC and GLK results agree. For higher frequencies, however, the GLK chi-factors are 2-3 times smaller than those given by DTC.

5.0 RECURSIVE RESIDUE GENERATION METHOD

5.1 General Description of the Method

RRGM is a nonperturbative method for constructing time dependent transition amplitudes that is particularly well-suited to problems with large, but sparse matrices.^{10,11} In this method, the Hamiltonian for the system is first tridiagonalized using the Lanczos Recursion Algorithm.¹⁷ Subsequent diagonalization of the tridiagonal (Jacobi) matrix yields the residues and eigenvalues needed to determine a given transition amplitude.

If $\{|\alpha\rangle\}$ and $\{E_\alpha\}$ are the eigenstates and eigenvalues of the Hamiltonian H , the time dependent transition amplitude between two nonstationary states $|i\rangle$ and $|f\rangle$ is

$$A_{fi}(t) = \langle f | e^{-iHt/\hbar} | i \rangle = \sum_{\alpha} \langle f | \alpha \rangle \langle \alpha | i \rangle e^{-iE_{\alpha}t/\hbar} = \sum_{\alpha} R_{fi}(\alpha) e^{-iE_{\alpha}t/\hbar} \quad (5-1)$$

where $R_{fi}(\alpha) = \langle f | \alpha \rangle \langle \alpha | i \rangle$ is the off diagonal residue corresponding to a simple pole E_{α} for the Green's function,

$$G_{fi}(\alpha) = \langle f | (z-H)^{-1} | i \rangle = \sum_{\alpha} \frac{\langle f | \alpha \rangle \langle \alpha | i \rangle}{z-E_{\alpha}} = \sum_{\alpha} \frac{R_{fi}(\alpha)}{z-E_{\alpha}} \quad (5-2)$$

For smaller systems the residues and eigenvalues needed to evaluate $A_{fi}(t)$ can be obtained by standard diagonalization methods. For larger systems, however, these procedures are usually prohibited by computer storage requirements. RRGM circumvents this difficulty because the actual eigenvectors are never explicitly generated.

It is easily shown that upon defining the vectors

$$|u_0\rangle = [|i\rangle + |f\rangle]/\sqrt{2} \quad (5-3a)$$

$$|v_0\rangle = [|i\rangle - |f\rangle]/\sqrt{2} \quad (5-3b)$$

the off-diagonal residue $R_{fi}(\alpha)$ can be expressed in terms of the diagonal residues associated with the vectors $|u_0\rangle$ and $|v_0\rangle$ as

$$\begin{aligned} R_{fi}(\alpha) &= \langle f | \alpha \rangle \langle \alpha | i \rangle = [\langle u_0 | \alpha \rangle \langle \alpha | u_0 \rangle - \langle v_0 | \alpha \rangle \langle \alpha | v_0 \rangle] / 2 \\ &= [R_{u_0, u_0}(\alpha) - R_{v_0, v_0}(\alpha)] / 2 \end{aligned} \quad (5-4)$$

In addition, if $|u_0\rangle$ is the first vector of a set of vectors $\{|u_i\rangle\}$ and $|v_0\rangle$ is the first vector in another orthonormal set of vectors $\{|v_i\rangle\}$, each of which tridiagonalizes the Hamiltonian H , i.e.

$$U^\dagger H U = J_u \quad (5-5a)$$

$$V^\dagger H V = J_v \quad (5-5b)$$

then the residues R_{u_0, u_0} and R_{v_0, v_0} can be determined by diagonalizing the Jacobi matrices J_v and J_u . Specifically, if T_u and T_v are the matrices which diagonalize J_u and J_v , respectively, then the needed residues are given by

$$R_{u_0, u_0}(\alpha) = (T_u)_{1, \alpha} (T_u)_{\alpha, 1} \quad (5-6a)$$

$$R_{v_0, v_0}(\alpha) = (T_v)_{1, \alpha} (T_v)_{\alpha, 1} \quad (5-6b)$$

It is important to note that only the first column of the T_u and T_v matrices are needed to determine all the residues and eigenvalues required to compute the transition amplitude A_{fi} .

Up to this point there has been no reduction in the computational requirements. Rather, the initial problem of diagonalizing the Hamiltonian H has simply been exchanged for the equally formidable problem (for larger systems) of determining the two Jacobi matrices. The key feature in RRG is that the columns of the transformation matrices U and V (as well as the diagonal and off-diagonal elements of J_u and J_v) are determined recursively using the Lanczos tridiagonalization algorithm¹⁷ so that only two columns of the complete matrices are required in fast storage. For example, starting with the initial recursion vector $|u_0\rangle$ and its self-energy $a_0 = \langle u_0 | H | u_0 \rangle$, the second vector in the set is defined by $|u_1\rangle = [(H - a_0) | u_0 \rangle] / b_1$ where b_1 is the norm of the so-called residual vector, $(H - a_0) | u_0 \rangle$. The self-energy a_0 and norm b_1 are the first diagonal and off-diagonal elements of J_u . Subsequent recursion vectors $|u_n\rangle$ and diagonal a_n and off-diagonal b_n elements of J_u are then determined by the three-term recursion relation

$$|u_{n+1}\rangle = [(H - a_n) | u_n \rangle - b_n | u_{n-1} \rangle] / b_{n+1} \quad (5-7)$$

where $a_n = \langle u_n | H | u_n \rangle$ and b_{n+1} normalizes the residual vector $[(H - a_n) | u_n \rangle - b_n | u_{n-1} \rangle]$. By construction, each recursion vector is implicitly orthogonal to all previous vectors. A second application of the Lanczos algorithm starting with $|v_0\rangle$ as the initial recursion vector yields the diagonal and off-diagonal matrix elements of J_v . Diagonalization of the two Jacobi matrices is straightforward and gives the residues in Equation (5-6).

To effectively realize the full potential of RRG, the Hamiltonian matrix must be relatively sparse and/or the intermolecular coupling matrix elements easily computed so that large amounts of storage are not required for coupling matrix elements. This indeed tends to be the case for the spectral line broadening problem for three reasons. First, the intermolecular interaction can often be represented by an expansion (e.g. multipole expansion or a numerical fit to a Legendre polynomial expansion) whose individual terms can be factored into components which act only on the subspaces for the separated

molecular/atomic species and their relative motion. Second, selection rules and/or conservation of total angular momentum further decrease the number of nonzero coupling matrix elements within a given subspace. Third, a portion of the interaction coupling resides entirely in the coupling of angular momenta and is easily computed in terms of Clebsch-Gordan coefficients and 6-j symbols. The net consequence is that although the coupling matrix elements are significantly more complicated for line broadening than in earlier applications of RRGH, the basic requirements for implementation of RRGH should be satisfied.

5.2 Application to HCl-Ar

As a preliminary test of the method, RRGH has been used to calculate the dipole autocorrelation function for the $j_i = 5 \rightarrow j_f = 6$ pure rotational line of a dilute HCl-Ar mixture. The HCl-Ar system has been previously treated by Boulet and Robert within a unified semiclassical theory using curved classical trajectories and including all orders in the inter-molecular interaction.¹⁸ The results from this latter method were used in comparisons against the RRGH results.

5.2.1 System Hamiltonian and Matrix Elements

In treating HCl-Ar rotational line broadening we have used the space-fixed Arthurs and Dalgarno¹⁹ rigid rotor theory for scattering of a structureless atom by a Σ -state rigid rotor diatomic. The coordinate system in this approach has its origin at the system center-of-mass and its axes aligned with space-fixed directions. The Hamiltonian, after separating out the center-of-mass motion, for a single radiator (HCl)--perturber (Ar) pair is

$$H = H_{\text{rad}} - \frac{\hbar^2}{2\mu} \vec{\nabla}^2 + V \quad (5-8)$$

where V is the Born-Oppenheimer intermolecular potential, ∇ is the Laplacian operator of R (vector between the atom and diatomic center-of-mass), μ is the reduced mass of Ar relative to HCl, and H_{rad} is the Hamiltonian for the nuclear motion of the radiator. Since we are interested in rotational line broadening, we will simplify the problem by neglecting the diatomic vibrational degree of freedom and treating HCl as a rigid rotor. The eigenfunctions of H_{rad} then satisfy

$$H_{\text{rad}} Y_{jm_j} = E_j Y_{jm_j} \quad (5-9)$$

where Y_{jm_j} is a spherical harmonic in the angular degrees-of-freedom of r , (θ_r, ϕ_r) . Similarly, if L is the angular momentum of Ar relative to HCl, then the eigenfunctions of the operator L^2 and L_z are $Y_{\ell, m_\ell}(\theta_R, \phi_R)$.

Since the total angular momentum $J = J_{\text{rad}} + L$ is conserved, it is convenient to couple Y_{jm_j} and Y_{ℓ, m_ℓ} to form eigenfunctions of J^2 , J_z , J_{rad}^2 and L^2 using the Clebsch-Gordan expansion

$$|j\ell JM\rangle = \sum_{m_j = -j}^j \sum_{m_\ell = -\ell}^{\ell} (jm_j \ell m_\ell | j\ell JM) |jm_j\rangle |\ell m_\ell\rangle \quad (5-10)$$

In addition, since RRGm relies on matrix operations, the translation continuum will be discretized by enclosing the atom-diatomic system in a sphere of radius R_0 . A spherical Bessel basis set,

$$x_n(R) = \eta \frac{2k_n^2}{R_0} \theta^{\frac{1}{2}} J_0(k_n R) = \eta \frac{2}{R_0} \theta^{\frac{1}{2}} \frac{\sin(k_n R)}{R} \quad (5-11)$$

$$k_n = \frac{n\pi}{R_0}$$

is then used to span the translational quasi-continuum.

In terms of these zero-order basis functions the Hamiltonian matrix elements are

$$\langle j' \ell' J' M' n' | H | j \ell J M n \rangle = \delta_{J' J} \delta_{M' M} \left[\left\{ \left(E_j + \frac{\hbar^2 \hbar^2}{8\mu R_0^2} \right) \delta_{n' n} + \right. \right. \quad (5-12)$$

$$\left. \frac{\hbar^2}{2\mu} \ell(\ell+1) \langle n' | R^{-2} | n \rangle \right\} \delta_{\ell' \ell} \delta_{j' j} + \langle j' \ell' J' M' n' | V | j \ell J M n \rangle]$$

If the intermolecular potential is expanded in Legendre polynomials

$$V(R, \theta) = \sum_{\lambda} V_{\lambda}(R) P_{\lambda}(\cos \theta) \quad (5-13)$$

then the coupling matrix elements for fixed total angular momentum J are

$$\langle j' \ell' J M n' | V | j \ell J M n \rangle = \sum_{\lambda} \langle n' | V_{\lambda}(R) | n \rangle f_{\lambda}(j' \ell'; j \ell; J) \quad (5-14)$$

where the f_{λ} are the Percival-Seaton coefficients²⁰

$$f_{\lambda}(j' \ell'; j \ell; J) = (-1)^{\ell_1 + \ell_2 + J} (j 0 j 0 | j j \lambda 0) (\ell' 0 \ell 0 | \ell' \ell \lambda 0) \times \quad (5-15)$$

$$[(2j'+1)(2\ell'+1)(2j+1)(2\ell+1)]^{\frac{1}{2}} \left\{ \begin{matrix} j' & \ell' & J \\ \ell & j & \lambda \end{matrix} \right\}$$

Several different potentials have been proposed to describe the HCl-Ar system. Typically, they are of the form given in Equation 5-13. In both our calculations and those of Boulet and Robert,¹⁸ the semiempirical "A₂" potential of Kircz et al.²¹ was used. In this case $\lambda = 0, 1$ and 2 and the radial potentials $V_{\lambda}(R)$ are 6-12 Lennard-Jones potentials whose parameters were obtained by fitting half-widths calculated using semiclassical S-matrix

theory to experimental measurements. These radial functions are displayed in Figure 5.1.

5.2.2 Dipole Autocorrelation Function

Since the Hamiltonian is diagonal in the total angular momentum (Eq. 5-12), the single-perturber dipole autocorrelation function

$$\Phi(\tau) = \text{Tr}[\vec{\mu} \{e^{iH\tau/\hbar} \vec{\mu} e^{-iH\tau/\hbar} \rho(H)\}] \quad (5-18)$$

can be expressed as a sum of terms corresponding to fixed initial and final total angular momentum. Specifically, for the $j_i \rightarrow j_f$ transition in the uncoupled line approximation and using the zero-order basis set defined in 5.1.1,

$$\Phi_{j_i j_f}(\tau) = (1/3) (-1)^{J_i + J_f} [(2j_i+1)(2j_f+1)]^{1/2} |\langle j_i | \mu | j_f \rangle|^2 \times \quad (5-19)$$

$$\sum_{J_i} \sum_{J_f} \Phi_{j_i j_f}^{J_i J_f}(\tau)$$

with

$$\Phi_{j_i j_f}^{J_i J_f}(\tau) = (2J_i+1) (2J_f+1) \sum_{\ell_i} \sum_{\ell_f} (-1)^{\ell_i + \ell_f} \left\{ \begin{matrix} J_i & j_i & \ell_i \\ j_f & J_f & 1 \end{matrix} \right\} \left\{ \begin{matrix} j_i & J_i & \ell_f \\ j_f & J_f & 1 \end{matrix} \right\} \times$$

$$\sum_{n_i} \sum_{n_f} \langle j_f \ell_i J_f n_i | e^{iH\tau/\hbar} | j_f \ell_f J_f n_f \rangle \langle j_i \ell_f J_i n_f | e^{-iH\tau/\hbar} e^{-\beta H} | j_i \ell_i J_i n_i \rangle \quad (5-20)$$

For comparison with the results of Boulet and Robert,¹⁸ it is necessary to relate the single perturber correlation function $\Phi(\tau)$ to the autocorrelation function for a dilute mixture $\Phi_{np}(\tau)$ where n_p is the perturber

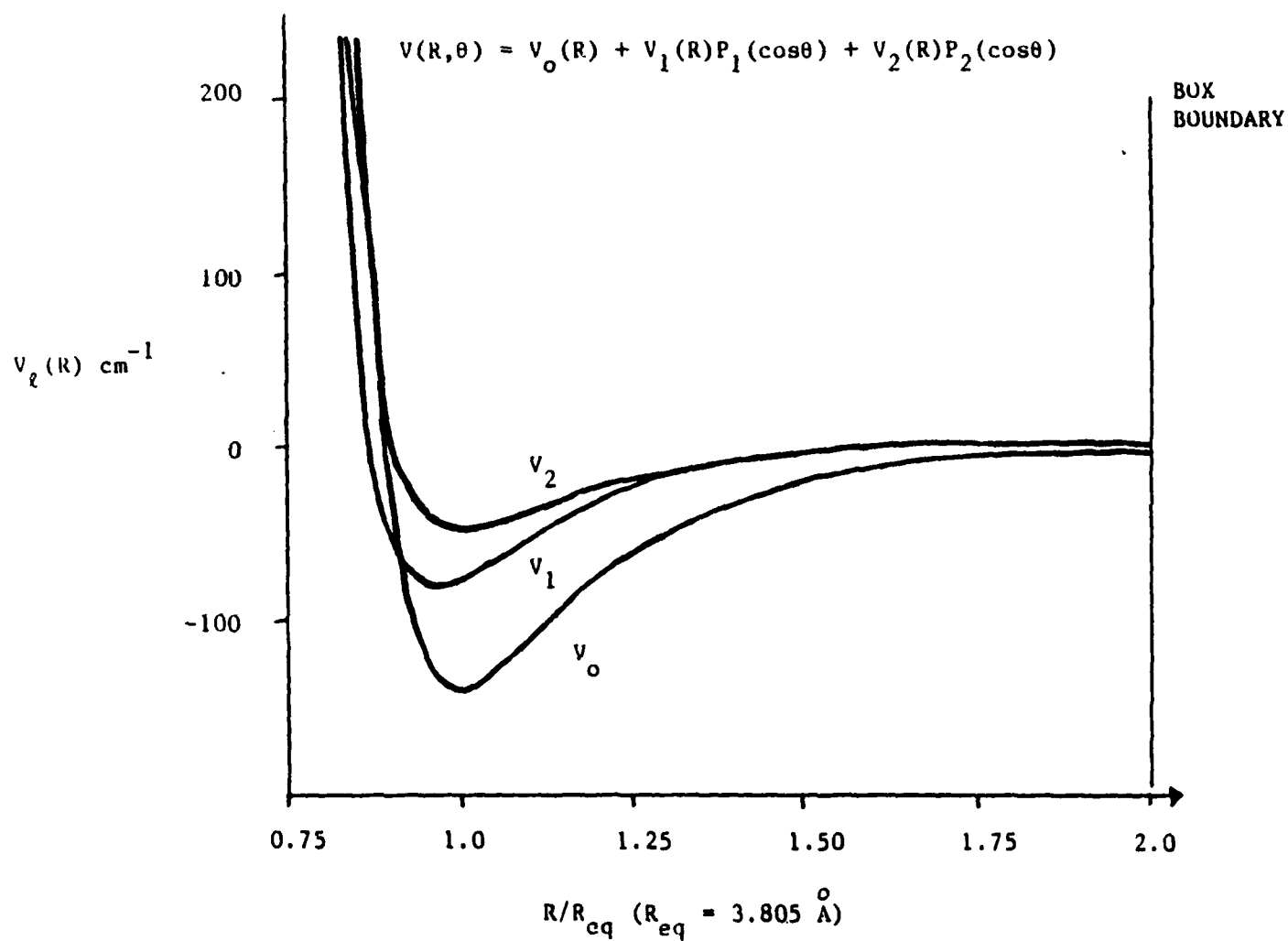


Figure 5.1. Radial Components of the Anisotropic Potential for HCl-Ar.

density. By analogy with DTC theory (Appendix A), this is accomplished by assuming that the autocorrelation function for N_p perturbors, $\Phi_{N_p}(\tau)$, is simply the product of N_p uncorrelated single-perturber distributions. Then,

$$\Phi_{N_p}(\tau) = \prod_p e^{i(E_f - E_i)\tau/\hbar} \Phi(\tau) = [e^{-i(E_f - E_i)\tau/\hbar} \Phi(\tau)]^{N_p} \quad (5-21)$$

where the complex exponential factor cancels out the zero-order time dependence from H_{rad} . Following normalization to unity at $t = 0$, Equation 5-21 should be equal to the normalized autocorrelation function in Reference 18, i.e.,

$$[e^{-i(E_f - E_i)\tau/\hbar} \Phi(\tau)]^{N_p} = e^{-n_p \sigma^3 \psi(\tau)} \quad (5-22)$$

or

$$\psi(t) = -\frac{\Omega}{3} \ln [e^{-i(E_f - E_i)\tau/\hbar} \Phi(\tau)] \quad (5-23)$$

where σ is the Lennard-Jones distance parameter and $\Omega = N_p/n_p$ is the system volume

$$\Omega = \frac{4\pi R_0^3}{3} \quad (5-24)$$

for a sphere of radius R_0 . In Equations 5-22 and 5-23, the "potential correlation function" $\psi(\tau)$ is defined as the average over velocity and impact parameter of the time evolution of initial and final zero-order states.

5.2.3 Preliminary Results

As a preliminary test of the RRGm method, $\psi(\tau)$ was initially calculated by assuming the diagonal transition ($l_i = l_f$ and $n_i = n_f$ in Equation 5-19) are the dominant contributors to the autocorrelation function at short times. The results from this calculation are shown in Figures 5.2 and 5.3 for times up to 1.0 and 0.4 ps, respectively. There is a clear discrepancy between the RRGm and French results, even for time less than 0.4 ps. Since our analysis of the convergence of the RRGm results with respect to the number of recursions indicates that our results should be accurate (at least up to about 0.4 ps), the discrepancies in Figure 5.3 probably result from a lack of convergence with respect to the size of the basis set and/or the neglect of off-diagonal transitions in Eq. (5-22).

Despite the discrepancies, there are also some encouraging features. Most notable is the indication of long time (impact) behavior starting at about 0.6 ps. The slope of the approximately linear long time tail for the RRGm results gives a halfwidth of 0.02 cm^{-1} which is in reasonably good agreement with experimental measurements. In addition, there is some indication that for times greater than about 0.2 - 0.3 ps only a relatively few transition amplitudes are contributing to the autocorrelation function. Significantly more transitions appear to contribute to the short time dynamics. However, these transitions can be treated quite accurately with just a few recursions. As a result, although a great amount of CPU time was expended in obtaining the RRGm results, intelligent optimization of the FORTRAN codes in terms of which transitions and corresponding numbers of recursions are used to compute the autocorrelation function could significantly decrease the required CPU time.

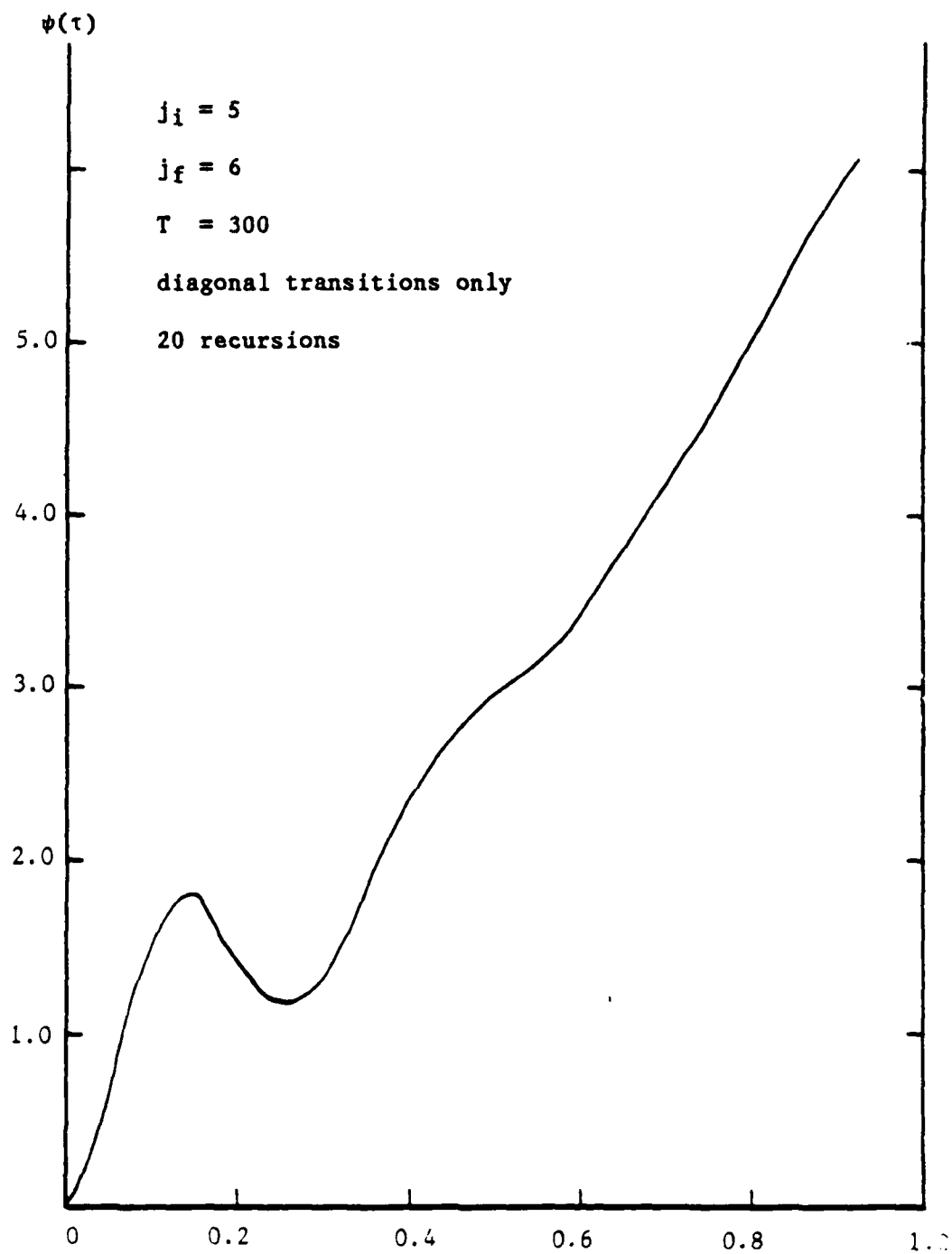


Figure 5.2. RRGm Potential Correlation Function for Ar-HCl at Longer Times.

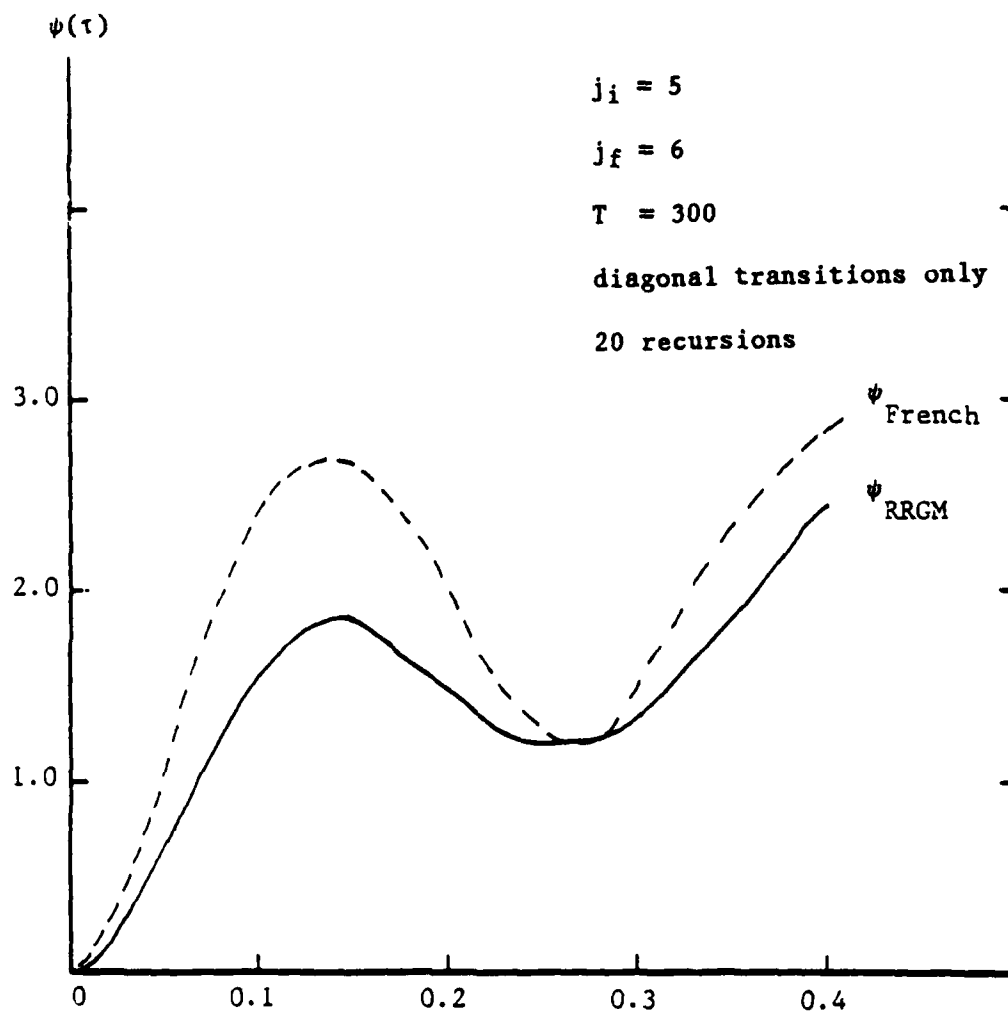


Figure 5.3. Potential Correlation Function for Ar-HCl from RRG M Calculation Compared to Result of Reference 1.

6.0 SUMMARY

Several critical military, geophysical, and energy related applications require accurate predictions of long path transmission in atmospheric window bands. Accurate predictions of transmission in these regions requires, in turn, more accurate characterization of far off resonance absorption line shapes than currently available. Accurate experimental absorption data is presently difficult to determine because of large experimental uncertainties. At the same time, theoretical approaches have typically been limited by severe computational (cpu time and storage) requirements.

This report has presented an analysis of two distinct approaches to the problem of calculating far wing absorption for collision induced broadening. The first approach uses standard time dependent perturbation theory to evaluate the time dependent, dipole autocorrelation function, followed by a frequency Fourier transform to give the absorption cross section. Two methods of this kind were evaluated which differed in the limit that perturbation theory broke down. The second approach evaluates the autocorrelation function nonperturbatively using the recursive residue generation method (RRGM).

The perturbation approaches closely resemble Anderson's impact theory for half-widths in that they are strictly valid only for weak interactions. These approaches do offer some improvement in principle, in that they treat all degrees of freedom quantum mechanically and satisfy the fluctuation dissipation theorem. In addition, although the Davies, Tipping, and Clough (DTC) method relies on ad-hoc, Anderson-like cutoff functions in the frequency domain to ensure physically well balanced absorption cross sections in strong collision regimes, the generalized Leavitt-Korff (GLK) method is cut-off free in the sense that the autocorrelation function remains well behaved as the impact parameter approaches zero.

The perturbation methods have been used to treat H₂O self broadening. H₂O absorption is particularly important in the 10 μ m region where absorption is thought to arise from line wings of the 6.3 μ m and pure rotation bands. Experimental measurements in this region indicate that the χ -factors (ratio of observed absorption to that predicted from Lorentzian line shapes) range from 0.1 to 0.6 and show a decrease with increasing temperature between 250 and 400 K.

Application of the DTC method to one of the stronger rotational lines of H₂O, (4,1,4) \rightarrow (505), gave χ -factors at 1000 cm⁻¹ which were approximately an order of smaller than experimental χ -factors at the same frequency. In addition, the calculated χ -factors showed a strong positive temperature dependence for 250 $\leq T \leq$ 400. The DTC results were based on multipole expansion up to and including dipole-quadrupole interactions. Higher order interactions would increase the χ -factors and may even change their temperature dependence. However, since multipole expansions often converge slowly, it is unclear to what extent these interactions would improve line wing behavior. Initial results (up to 400 cm⁻¹) from the GLK method tended to differ from DTC χ -factors further off resonance. This difference was not large enough to cause us to suspect any significant change in the temperature dependence.

Analysis of our results suggest two conclusions. First, a multipole expansion of the anisotropic electrostatic interaction is probably insufficient to accurately characterize far wing absorption for self-broadened H₂O. Second, strong collisions contribute to the absorption up to 1000 cm⁻¹ off line center. The calculated absorption strengths can differ significantly depending upon the approximations or cut-off functions used to ensure physically reasonable absorption cross sections in strong collision regions.

Based on these conclusions, the RRGGM was explored as a possible approach to line broadening. RRGGM is a nonperturbative method which can treat more general interactions than the typical multipole expansion. As part of an initial feasibility study, the method was used in a restricted context to determine HCl-Ar line wings. In general the results were encouraging but more work is required for applications to systems of atmospheric interest.

7.0 REFERENCES

1. A. Deepak, T.D. Wikerson and L.H. Ruhnke, Atmospheric Water Vapor, Academic Press, New York (1980).
2. R.E. Roberts, J.E.A. Selby and L.M. Biberman, Appl. Opt. 15, 2085 (1976).
3. R.W. Davies, R.H. Tipping and S.A. Clough, "Dipole Autocorrelation Function Formulation for Molecular Pressure Broadening," Phys. Rev. A 26, 3378 (1982).
4. R.W. Davies and S.F. Fahey, "Calculation of H₂O Far Wing Absorption Within the Single-Perturber Approximation," AFGL-TR-85-0033 (February 1985, ADA160405).
5. T.F. George and J. Ross, "Quantum Dynamical Theory of Molecular Collisions," Ann. Rev. Phys. Chem. 24, 263 (1973).
6. D. Secrest, "Theory of Rotational and Vibrational Energy Transfer in Molecules," Ann. Rev. Phys. Chem. 24, 379 (1973).
7. J.F. Kielkopf and J.A. Gwinn, "Semiclassical Theory of Satellite Bands Produced in the Spectra of Alkali Metals by Interaction with Foreign Gases," J. Chem. Phys. 48, 5570 (1968).
8. K.M. Sando and P.S. Herman, "Detailed Balance Theory of Pressure-Broadening of Atomic Lines," in Spectral Line Shapes, Vol. 2, pg. 497 (Walter de Gruyter and Co., Berlin), 1983.
9. R.P. Leavitt and D. Korff, "Cutoff-Free Theory of Impact Broadening and Shifting in Microwave and Infrared Gas Spectra," J. Chem. Phys. 74, 2180 (1981).
10. André Nauts and R.E. Wyatt, "New Approach to Many-State Quantum Dynamics: The Recursive-Residue-Generation Method," Phys. Rev. Lett. 51, 2238 (1983).
11. André Nauts and R.E. Wyatt, "Theory of Laser-Molecule Interaction: The Recursive-Residue-Generation Method," Phys. Rev. A 30, 872 (1984).
12. G. Birnbaum and E.R. Cohen, "Theory of Line Shape in Pressure-Induced Absorption," Can. J. Phys. 54, 593 (1976).

13. S.A. Clough, F.X. Kneizys, R. Davies, R. Gamache and R. Tipping, "Theoretical Line Shape for H₂O Vapor; Application to the Continuum," AFGL-TR-81-0283, ADA105419.
14. P. Varanasi and S. Chudamani, "Self- and N₂-Broadened Spectra of Water Vapor Between 7.5 and 14.5 μ m," J. Quant. Spectrosc. Radiat. Transfer 38, 407 (1987).
15. D.E. Burch and D.A. Gryvnak, "Continuum Absorption by H₂O Vapor in the Infrared and Millimeter Regions," in Reference 1.
16. P.W. Anderson, "Pressure Broadening in the Microwave and Infra-Red Regions," Phys. Rev. 76, 647 (1949).
17. C. Lanczos, J. Res. Natl. Bur. Stand. 45, 255 (1950).
18. C. Boulet and D. Robert, "Short Time Behavior of the Dipole Autocorrelation Function and Molecular Gases Absorption Spectrum," J. Chem. Phys. 77, 4288 (1982).
19. A.M. Arthurs and A. Dalgarno, "The Theory of Scattering by a Rigid Rotator", Proc. R. Soc. Lond. A 256, 540 (1960).
20. I.C. Percival and M.J. Seaton, "The Partial Wave Theory of Electron-Hydrogen Atom Collisions," Proc. Camb. Phil. Soc. 53, 654 (1957).
21. J.G. Kircz, G.J.Q. van der Peyl, and J. van der Elsken, "Determination of Potential Energy Surfaces for Ar-HCl and Kr-HCl from Rotational Line Broadening Data," J. Chem. Phys. 69, 4606 (1978).
22. J.K. Cashion, J. Chem. Phys. 39, 1872 (1963).
23. Handbook of Mathematical Functions, Edited by M. Abramowitz and I. Stegun, National Bureau of Standards, Applied Mathematics Series 55, Fourth Printing (December 1965).
24. R.P. Leavitt, "An Irreducible Tensor Method of Defining the Long-range Anisotropic Interactions Between Molecules of Arbitrary Symmetry," J. Chem. Phys. 72, 3472 (1980).
25. A.D. Buckingham, Adv. Chem. Phys. 12, 107 (1967).

APPENDIX A.

DERIVATION OF DAVIES, TIPPING, AND CLOUGH LINESHAPE FUNCTION

The time evolution in Eq. (2-4) can be treated using standard time dependent perturbation theory by first partitioning the Hamiltonian into zeroth-order and perturbative terms

$$H = H_0 + V \quad (\text{A-1})$$

and then defining the time evolution operator $U(z)$ by

$$e^{-iHz/\hbar} = e^{-iH_0 z/\hbar} U(z) \quad (\text{A-2a})$$

$$e^{+iHz/\hbar} U^\dagger(z) = e^{iH_0 z^*/\hbar} \quad (\text{A-2b})$$

The operator $U(z)$ satisfies the integral equation

$$U(z) = 1 - \int_0^z V(z') U(z') dz' \quad (\text{A-3})$$

$$V(z) = e^{iH_0 z/\hbar} V e^{-iH_0 z/\hbar} \quad (\text{A-4})$$

subject to the initial condition that $U(0) = 1$. Eq. (A-3) can be solved iteratively to give the usual perturbative series, i.e.

$$U(z) = \sum_{n=0}^{\infty} \left(-\frac{i}{\hbar}\right)^n \int_0^z dz_1 \dots \int_0^{z_{n-1}} [V(z_1) V(z_2) \dots V(z_n)] dz_n \quad (\text{A-5})$$

In DTC theory,³ H_0 represents the zeroth-order Hamiltonian for the isolated molecules plus the kinetic energy operators for their relative motion and any isotropic intermolecular interactions, while the perturbation V

represents the anisotropic interactions which do not commute with H_0 . The zeroth-order Hamiltonian can then be further decomposed as

$$H_0 = H_R^0 + \tilde{H}_0 \quad (A-6)$$

where H_R^0 is the molecular Hamiltonian for the radiator and \tilde{H}_0 contains the remaining zeroth-order terms. Here we will neglect vibration-rotational interactions and take H_R^0 to be the Hamiltonian for a rigid rotor with eigenstates

$$H_R^0 | j\tau m \rangle = E_{j\tau} | j\tau m \rangle \quad (A-7)$$

where j is the total angular momentum, m is the projection on the quantization axis and τ represents any additional quantum numbers needed to completely specify the rotational state.

Performing the trace over radiator states in Eq. (2-4) and using the Wigner-Eckart theorem to evaluate the dipole matrix elements, the autocorrelation function becomes

$$\begin{aligned} \phi(t) = \frac{\rho_0}{\rho_p} \sum_i \sum_f \sum_{i'} \sum_{f'} (2j_i + 1) \rho(E_i) < j_i \tau_i \| \mu \| j_f \tau_f > \quad (A-8) \\ \times < j_f' \tau_f' \| \mu \| j_i' \tau_i' > e^{i\omega_{f'i'} t} C_{ii',ff'}^{(\tau)} \end{aligned}$$

where

$$C(t)_{ii',ff'} = (2j_i + 1)^{-1} \sum_{m_i} \sum_{m_f} \sum_{m_i'} \sum_{m_f'} \sum_m (j_f, m_f, 1, m | j_f, 1, j_i, m_i) \\ (j_f', m_f', 1, m | j_f', 1, j_i', m_i') \times \tilde{\text{Tr}} [\rho(\tilde{H}_0)] \quad (\text{A-9})$$

$$< j_i' \tau_i' m_i' | U(z) | j_i \tau_i m_i > < j_f \tau_f m_f | U^+(\tau) | j_f' \tau_f' m_f' >]$$

and

$$\rho(E)_i = \frac{e^{-\beta E_i}}{\text{Tr}[e^{-\beta H_R^0}]} = \frac{e^{-\beta E_i}}{Q_R^0} \quad (\text{A-10a})$$

$$\rho(\tilde{H}_0) = \frac{e^{-\beta \tilde{H}_0}}{\tilde{\text{Tr}}[e^{-\beta \tilde{H}_0}]} = \frac{e^{-\beta \tilde{H}_0}}{\tilde{Q}_p^0} \quad (\text{A-10b})$$

are the canonical density matrices for the zeroth-order Hamiltonians H_R and \tilde{H}_0 and $\tilde{\text{Tr}}$ is the quantum mechanical trace associated with \tilde{H}_0 .

For sufficiently low perturber densities, it has been shown that many spectral features can be reproduced, at least qualitatively, by invoking the binary collision approximation. In this approximation, the N_p -perturber autocorrelation function is taken to be the simple uncorrelated product of single perturber autocorrelation functions. Equation (A-9) then becomes

$$C(t)_{ii',ff'} = [Q(t)_{ii',ff'}]^{N_p} \quad (\text{A-11})$$

where

$$Q(t)_{ii',ff'} = (2j_i + 1)^{-1} \sum_m \sum_{m_i} \sum_{m_f} \sum_{m_i'} \sum_{m_f'} (j_f, m_f, 1, m | j_f, 1, j_i, m_i) \\ (j_f', m_f', 1, m | j_f', 1, j_i', m_i') \times \tilde{\text{Tr}} [\rho(H_0^S)] \quad (\text{A-12})$$

$$< j_i' \tau_i' m_i' | U_s(z) | j_i \tau_i m_i > < j_f \tau_f m_f | U_s^+(t) | j_f' \tau_f' m_f' >]$$

is the autocorrelation function for the interaction between the radiator and a single perturber (designated by the subscript or superscript s).

The single perturber autocorrelation function given in Equation (4-12) includes line coupling effects. When the zeroth-order absorption lines are well separated, however, the calculation can be simplified considerably by invoking the uncoupled line approximation. In the present context, the uncoupled line approximation is

$$Q(t)_{ii',ff'} \approx \delta_{ii'} \delta_{ff'} Q(t)_{if} \quad (\text{A-13})$$

where $Q_{if}(t)$ is given by

$$Q(t)_{if}^{-1} = (2j_i + 1) \sum_m \sum_{m_i} \sum_{m_f} \sum_{m_i'} \sum_{m_f'} (j_f, m_f, 1, m | j_f, 1, j_i, m_i) \\ \times (j_f', m_f', 1, m | j_f', 1, j_i', m_i') \times \tilde{\text{Tr}} [\rho(H_0^S)] \quad (\text{A-14}) \\ < j_i \tau_i m_i | U_s(z) | j_i \tau_i m_i > < j_f \tau_f m_f | U_s^+(t) | j_f \tau_f m_f >]$$

Either $Q_{ii,ff}(t)$ or $Q_{if}(t)$ is evaluated in DTC theory by substituting the perturbation series, Equation (A-5), for $U(z)$ and $U(t)$ and keeping only terms up to second order in the interaction. This procedure breaks down, however, for strong collisions leading to values for the autocorrelation function which are not physically reasonable. Consequently, in applications it is necessary to introduce cutoff functions which ensure that the correlation functions are always well behaved. In general, there is no formal basis for these functions.

APPENDIX B

COUPLING MATRIX ELEMENTS OF THE LONG RANGE ANISOTROPIC INTERACTION

In this appendix we determine the coupling matrix elements of the long range anisotropic interaction V between two molecules in an uncoupled basis set

$$|\alpha\rangle = |\alpha_1\rangle |\alpha_2\rangle |\ell m_\ell\rangle |\ell \epsilon\rangle \quad (\text{B-1})$$

consisting of molecular eigenfunctions for the internal degrees-of-freedom for each molecule

$$|\alpha_1\rangle = |\gamma_1 j_1 m_1\rangle \quad (\text{B-2a})$$

$$|\alpha_2\rangle = |\gamma_2 j_2 m_2\rangle \quad (\text{B-2b})$$

a spherical harmonic $|\ell m_\ell\rangle$ for the relative angular momentum, and radial eigenfunctions $|\ell \epsilon\rangle$ for the relative translational motion. Following a brief discussion of the long range electrostatic interaction desired by Leavitt,¹³ the Q functions (the squares of matrix elements of V summed over all magnetic quantum numbers) which arise in a perturbative treatment of line broadening are derived for arbitrary orders in a multipolar expansion of V .

We start with the electrostatic interaction given by Leavitt²⁴ for two charge distributions separated by a distance R

$$V = \sum_{\ell_1} \sum_{\ell_2} (-1)^{\ell_2} \binom{2\ell_1 + 2\ell_2}{2\ell_1}^{\frac{1}{2}} / R^{\ell_1 + \ell_2 + 1} \quad (B-3)$$

$$\times \sum_{\mu_1} \sum_{\mu_2} (\ell_1, \mu_1, \ell_2, \mu_2 | \ell_1, \ell_2, \ell_1 + \ell_2, \mu_1 + \mu_2) Q_{\ell_1, \mu_1}^{(1)} Q_{\ell_2, \mu_2}^{(2)} C_{\ell_1 + \ell_2, \mu_1 + \mu_2}^+(\hat{R})$$

where $Q_{\ell_1, \mu_1}^{(1)}$ and $Q_{\ell_2, \mu_2}^{(2)}$ are multipolar moment operators for the molecular systems 1 and 2, respectively, and C^+ is the adjoint of the irreducible spherical tensor given by

$$C_{\ell, \mu}(\hat{R}) = \left[\frac{4\pi}{(2\ell+1)} \right]^{\frac{1}{2}} Y_{\ell, \mu}(\hat{R}) \quad (B-4)$$

where $Y_{\ell, \mu}(\hat{R})$ is an ordinary spherical harmonic. The factor of the form $\binom{a}{b}$ is the binomial coefficient $a!/b!(a-b)!$ and $(a, \alpha, b, \beta | a, b, d, \delta)$ is the Clebsch-Gordan coefficient for the vector coupling of a and b to give the resultant d . If \vec{r}_{1i} and \vec{r}_{2j} are position vectors for charges q_i and q_j in charge distributions 1 and 2, then the moment operators are given by

$$Q_{\ell_1, \mu_1}^{(1)} = \sum_i q_i r_{1i}^{\ell_1} C_{\ell_1, \mu_1}(\hat{r}_{1i}) \quad (B-5a)$$

$$Q_{\ell_2, \mu_2}^{(2)} = \sum_j q_j r_{2j}^{\ell_2} C_{\ell_2, \mu_2}(\hat{r}_{2j}) \quad (B-5b)$$

As used in Equation (A-3), the multipolar moment operators are each defined relative to the laboratory reference frame. The spherical harmonic $Y_{\ell, \mu}$ then specifies the orientation of the \hat{R} vector relative to the laboratory z -axis.

The electrostatic interaction given in Equation (A-3), is invariant to the simultaneous rotation of all particles in the system. Most earlier expressions for the electrostatic multipolar interaction²⁵ require the application of rotation matrices to arrive at an equivalent form. This invariance is easily seen by noting that upon letting $\mu = \mu_1 + \mu_2$, the summation over μ_1 and μ_2 becomes

$$\sum_{\mu_1} \sum_{\mu_2} [\dots] = \sum_{\mu} C_{\ell_1}^{+(\hat{R})}{}_{+\ell_2, \mu} \sum_{\mu_1} (\ell_1, \mu_1, \ell_2, \mu - \mu_1 | \ell_1, \ell_2, \ell_1 + \ell_2, \mu) Q_{\ell_1, \mu_1}^{(1)} Q_{\ell_2, \mu - \mu_1}^{(2)}$$

The summation over μ_1 corresponds to the contraction of the multipole tensors Q_{ℓ_1, μ_1} and Q_{ℓ_2, μ_2} of order ℓ_1 and ℓ_2 in the molecular spaces 1 and 2, into a tensor $Q_{\ell_1 + \ell_2, \mu}$ of order $\ell_1 + \ell_2$ in both spaces. Then using

$$C_{\ell, \mu}^{+(\hat{R})} = (-1)^{\mu} C_{\ell, -\mu}(\hat{R}) \quad (\text{B-7})$$

the summation over μ corresponds to a scalar product to give a rotational invariant in the spaces 1, 2 and R, i.e.,

$$\sum_{\mu_1} \sum_{\mu_2} [\dots] = \sum_{\mu} (-1)^{\mu} Q_{\ell_1 + \ell_2, \mu}^{(1,2)} C_{\ell_1 + \ell_2, -\mu}(\hat{R}) = Q_{o,o}^{(1,2,\hat{R})} \quad (\text{B-8})$$

The matrix elements of V in the uncoupled basis set, Equation (B-2), are

$$V_{\alpha'\alpha} = \langle \alpha' | V | \alpha \rangle \quad (B-9)$$

$$= \sum_{\ell_1} \sum_{\ell_2} (-1)^{\ell_2} \begin{pmatrix} 2\ell_1 + 2\ell_2 \\ 2\ell_1 \end{pmatrix}^{\frac{1}{2}} \langle \ell' \ell' | R^{-(\ell_1 + \ell_2 + 1)} | \ell \ell \rangle$$

$$\times \sum_{\mu_1} \sum_{\mu_2} (\ell_1, \mu_1, \ell_2, \mu_2 | \ell_1, \ell_2, \ell_1 + \ell_2, \mu_1 + \mu_2) \langle \ell' j_1' m_1' | Q_{\ell_1, \mu_1}^{(1)} | \ell j_1 m_1 \rangle$$

$$\times \langle \ell' j_2' m_2' | Q_{\ell_2, \mu_2}^{(2)} | \ell j_2 m_2 \rangle \langle \ell' m_{\ell'} | C_{\ell_1 + \ell_2, \mu_1 + \mu_2}^+ | \ell m_{\ell} \rangle$$

If the Wigner-Eckart theorem is applied to the matrix elements of Q_{ℓ_1, μ_1} , Q_{ℓ_2, μ_2} and $C_{\ell_1 + \ell_2, \mu_1 + \mu_2}$,

$$\langle \ell' j_1' m_1' | Q_{\ell_1, \mu_1} | \ell j_1 m_1 \rangle = (j_1, m_1, \ell_1, \mu_1 | j_1, \ell_1, j_1', m_1') \quad (B-10a)$$

$$\times \langle \ell' j_1' || Q_{\ell_1}^{(1)} || \ell j_1 \rangle$$

$$\langle \ell' j_2' m_2' | Q_{\ell_2, \mu_2} | \ell j_2 m_2 \rangle = (j_2, m_2, \ell_2, \mu_2 | j_2, \ell_2, j_2', m_2') \quad (B-10b)$$

$$\times \langle \ell' j_2' || Q_{\ell_2}^{(2)} || \ell j_2 \rangle$$

$$\langle \ell' m_1' | C_{\ell_1 + \ell_2, \mu_1 + \mu_2}^+ | \ell m_\ell \rangle = (-1)^{\mu_1 + \mu_2} \langle \ell' m_1' | C_{\ell_1 + \ell_2, \mu_1 + \mu_2} | \ell m_\ell \rangle$$

$$= (-1)^{\mu_1 + \mu_2} \frac{\ell + 1}{\ell' + 1}^{\frac{1}{2}} (\ell, m_\ell, \ell_1 + \ell_2, -(\mu_1 + \mu_2) | \ell, \ell_1 + \ell_2, \ell', m_\ell')$$

$$\times (\ell, 0, \ell_1 + \ell_2, 0 | \ell, \ell_1 + \ell_2, \ell', 0) \quad (B-10c)$$

the matrix elements of V become

$$V_{\alpha' \alpha} = \sum_{\ell_1 \ell_2} A_{\ell_1 \ell_2} B_{\ell_1 \ell_2} \quad (B-11)$$

where

$$A_{\ell_1 \ell_2} = (-1)^{\ell_2} \left(\frac{2\ell_1 + 2\ell_2}{2\ell_1} \right)^{\frac{1}{2}} \langle \ell' \epsilon' | R^{-(\ell_1 + \ell_2 + 1)} | \ell \epsilon \rangle \quad (B-12)$$

$$\times \langle \gamma_1' j_1' | | Q_{\ell_1}^{(1)} | | \gamma_1 j_1 \rangle \langle \gamma_2' j_2' | | Q_{\ell_2}^{(2)} | | \gamma_2 j_2 \rangle$$

$$\times (\ell, 0, \ell_1 + \ell_2, 0 | \ell, 0, \ell_1 + \ell_2, \ell', 0)$$

and

$$B_{\ell_1 \ell_2} = \sum_{\mu_1} \sum_{\mu_2} (\ell_1, \mu_1, \ell_2, \mu_2 | \ell_1, \ell_2, \ell_1 + \ell_2, \mu_1 + \mu_2) \quad (B-13)$$

$$\times (\ell, m_\ell, \ell_1 + \ell_2, -(\mu_1 + \mu_2) | \ell_1, \ell_1 + \ell_2, \ell', m'_\ell)$$

$$\times (j_1, m_1, \ell_1, \mu_1 | j_1, \ell_1, j'_1, m'_1)$$

$$\times (j_2, m_2, \ell_2, \mu_2 | j_2, \ell_2, j'_2, m'_2)$$

where the factor $A_{\ell_1 \ell_2}$ is independent of magnetic quantum numbers.

For a perturbative treatment of line broadening, we are particularly interested in the rotationally invariant quantities

$$Q = \sum_{m_1} \sum_{m_1'}, \sum_{m_2} \sum_{m_2'}, \sum_{m_\ell} \sum_{m_\ell'} |v_{\alpha', \alpha}|^2 \quad (B-14)$$

which upon substituting Equation (A-11) becomes

$$Q = \sum_{\ell_1} \sum_{\ell_2} \sum_{\ell'_1} \sum_{\ell'_2} A_{\ell_1 \ell_2} A_{\ell'_1 \ell'_2}^* \sum_{\bar{m}} \sum_{\bar{m}'} B_{\ell_1 \ell_2}^* B_{\ell'_1 \ell'_2} \quad (B-15)$$

where \bar{m} refers to the set of magnetic quantum numbers (m_1, m_2, m_ℓ)

Substituting Equation (A-13) for $B\ell_1\ell_2$, the summation over \bar{m} and \bar{m}' is

$$\begin{aligned}
 & \sum_{\mu} \sum_{\mu} \sum_{\mu_1'} \sum_{\mu_2'} (-1)^{\mu_1+\mu_2} (-1)^{\mu_1'+\mu_2'} (\ell_1, \mu_1, \ell_2, \mu_2 | \ell_1, \ell_2, \ell_1+\ell_2, \mu_1+\mu_2) \\
 & (\ell_1', \mu_1', \ell_2', \mu_2' | \ell_1', \ell_2', \ell_1'+\ell_2', \mu_1'+\mu_2') \\
 & \times \sum_{m_\ell} \sum_{m_\ell'} (\ell, m_\ell, \ell_1+\ell_2, \mu_1+\mu_2 | \ell, \ell_1+\ell_2, \ell', m_\ell') \\
 & \times (\ell, m_\ell, \ell_1'+\ell_2', \mu_1'+\mu_2' | \ell, \ell_1', \ell_2', \ell', m_\ell') \\
 & \times \sum_{m_2} \sum_{m_2'} (j_2, m_2, \ell_2, \mu_2 | j_2, \ell_2, j_2', m_2') (j_2, m_2, \ell_2', \mu_2' | j_2, \ell_2', j_2', m_2') \\
 & \times \sum_{m_1} \sum_{m_1'} (j_1, m_1, \ell_1, \mu_1 | j_1, \ell_1, j_1', m_1') (j_1, m_1, \ell_1', \mu_1' | j_1, \ell_1', j_1', m_1') \quad (B-16)
 \end{aligned}$$

Using the Clebsch-Gordan symmetry relations, the summations over \bar{m}_1 and \bar{m}_1' are easily evaluated to give

$$\begin{aligned}
\sum_{m_1} \sum_{m'_1} [\dots] &= \frac{(2j_1+1)}{[(2\ell_1+1)(2\ell'_1+1)]^{\frac{1}{2}}} \sum_{m_1} \sum_{m'_1} (j_1, m_1, j'_1, -m'_1 | j_1, j'_1, \ell_1, -\mu_1) \quad (\text{B-17a}) \\
&\quad \times (j_1, m_1, j'_1, -m'_1 | j_1, j'_1, \ell'_1, -\mu'_1) \\
&= \frac{(2j_1+1)}{[(2\ell_1+1)(2\ell'_1+1)]^{\frac{1}{2}}} \delta_{\ell_1, \ell'_1} \delta_{\mu_1, \mu'_1}
\end{aligned}$$

Similarly, the summations over m_2, m'_2 and m_ℓ, m'_ℓ are

$$\sum_{m_2} \sum_{m'_2} [\dots] = \frac{(2j_1+1)}{[(2\ell_1+1)(2\ell'_1+1)]^{\frac{1}{2}}} \delta_{\ell_2, \ell'_2} \delta_{\mu_2, \mu'_2} \quad (\text{B-17b})$$

$$\sum_{m_\ell} \sum_{m'_\ell} [\dots] = \frac{(2\ell'+1)}{[(2\ell_1+2\ell_2+1)(2\ell'_1+2\ell'_2+1)]^{\frac{1}{2}}} \delta_{\ell_1+\ell_2, \ell'_1+\ell'_2} \delta_{\mu_1+\mu_2, \mu'_1+\mu'_2} \quad (\text{B-17c})$$

so that the summation over \bar{m} and \bar{m}' reduces to

$$\begin{aligned}
&\frac{(2j_1+1)(2j_2+1)(2\ell'+1)}{(2\ell_1+1)(2\ell_2+1)(2\ell_1+2\ell_2+1)} \delta_{\ell_1, \ell'_1} \delta_{\ell_2, \ell'_2} \quad (\text{B-18}) \\
&\quad \times \sum_{\mu_1} \sum_{\mu_2} (\ell_1, \mu_1, \ell_2, \mu_2 | \ell_1, \ell_2, \ell_1+\ell_2, \mu_1+\mu_2) (\ell_1, \mu_1, \ell_2, \mu_2 | \ell_1, \ell_2, \ell_1+\ell_2, \mu_1+\mu_2) \\
&= \frac{(2j_1+1)(2j_2+1)(2\ell'+1)}{(2\ell_1+1)(2\ell_2+1)} \delta_{\ell_1, \ell'_1} \delta_{\ell_2, \ell'_2}
\end{aligned}$$

Then substituting back into Equation (A-15) and performing the summations over ℓ_1' and ℓ_2' , we find

$$Q = \sum_{\ell_1} \sum_{\ell_2} \frac{(2j_1+1)(2j_2+1)(2\ell'+1)}{(2\ell_1+1)(2\ell_2+1)} |A_{\ell_1, \ell_2}|^2 \quad (B-19)$$

$$= \sum_{\ell_1} \sum_{\ell_2} \frac{\binom{2\ell_1+2\ell_2}{2\ell_1}}{(2\ell_1+1)(2\ell_2+1)} \cdot (2j_1+1)(2j_2+1)(2\ell'+1) (\ell, 0, \ell_1+\ell_2, 0 | \ell, \ell_1+\ell_2, \ell', 0)^2$$

$$\propto | \langle \ell' \ell' | R^{-(\ell_1+\ell_2+1)} | \ell \ell \rangle |^2 | \langle \gamma_1' j_1' | | Q_{\ell_1}^{(1)} | | \gamma_1 j_1 \rangle |^2 | \langle \gamma_2' j_2' | | Q_{\ell_2}^{(2)} | | \gamma_2 j_2 \rangle |^2$$

APPENDIX C

RADIAL MATRIX ELEMENTS OF $R^{-\lambda}$

When the anisotropic interaction potential is expressed as an expansion in multipolar moment operators for the radiator and perturber, the coupling matrix elements will include radial factors of the form

$$I_{\ell', \epsilon', \ell \epsilon}^{\lambda} = \langle \Psi_{\ell', \epsilon'} | R^{-(\lambda+1)} | \Psi_{\ell \epsilon} \rangle \quad (C-1)$$

where λ is the sum of the orders of the multipole tensor operators for the radiator and perturber and $\Psi_{\ell \epsilon}$ are radial eigenfunctions with energy,

$$\epsilon = \frac{\hbar^2 k^2}{2\mu}$$

In general, the eigenfunctions and integral in Equation (B-1) may be determined by numerical integration (method 1 below). However, the computation time may be reduced by using suitable approximations to the eigenfunctions in the limits $k^2 > \ell(\ell+1)/\rho_R^2$ (hard core regime) and $k^2 < \ell(\ell+1)/\rho_R^2$ (centripetal regime) where ρ_R is the radius of the interaction region of the isotropic potential. The three basic methods used to evaluate Equation (B-1) are summarized below. This discussion follows closely the description given in the DTC final report,⁴ but has been generalized where applicable to arbitrary values of λ .

Method 1: Numerical Integration

In the current source code MATRIX, as well as the previous GTE code OVERLAP, the eigenfunctions $\Psi_{\ell \epsilon}(R)$ are evaluated at a series of equally spaced grid points by numerically solving Schrodinger's equation using Numerov's method.²² The integral in Equation (B-1) is then evaluated using a

simple trapezoidal or Simpson numerical quadrature. Typically, the radial grid extends from $R = 0$ out to $R = R_{\max}$ such that

$$R_{\max}^{-(\lambda_{\min} + 1)} < \text{tol}$$

where tol is a user specified tolerance and λ_{\min} corresponds to the lowest order (longest range) interaction, e.g., dipole-dipole for two asymmetric rotors.

Method 2: Approximate Eigenfunction in the Hard Core Regime

In the limit $R \rightarrow \infty$, the eigenfunctions have the form

$$\Psi_{\ell\epsilon}(R) \underset{R \rightarrow \infty}{\sim} \frac{\sin [kR - \ell\pi/2 + \delta_{\ell}(k)]}{R} \quad (\text{C-2})$$

where $\delta_{\ell}(k)$ is an energy dependent phase shift.

At energies sufficiently large relative to the centripetal barrier (i.e., $k^2 > \ell(\ell+1)/\rho_R^2$), the radial wavefunctions approach their asymptotic sinusoidal form relatively close to the classical turning point on the repulsive wall. Defining R_a as the radial position at which the asymptotic limit is approximately valid for a given pair of wavefunctions, Equation (B-1) may be written as

$$I_{\ell'\epsilon',\ell\epsilon}^{\lambda} = \int_0^{R_a} dR R^2 \frac{\Psi_{\ell'\epsilon'}^* \Psi_{\ell\epsilon}}{R^{\lambda+1}} + A_{I_{\ell'\epsilon',\ell\epsilon}^{\lambda}} \quad (\text{C-3})$$

where the asymptotic contribution to the matrix element is given by

$$A_{I_{\ell', \varepsilon', \ell \varepsilon}}^{\lambda} = \int_{R_a}^{\infty} dR \frac{\sin(k'R + \theta') \sin(kR + \theta)}{R^{\lambda+1}} \quad (C-4)$$

and $\theta = \delta_{\ell}(k) - \ell\pi/2$

The asymptotic integration may be easily evaluated for arbitrary λ as follows.

If we define generalized sine and cosine integrals

$$I_m^C(k, \theta, x) = \int_x^{\infty} \frac{\cos(kR + \theta)}{R^m} dR \quad (C-5)$$

$$I_m^S(k, \theta, x) = \int_x^{\infty} \frac{\sin(kR + \theta)}{R^m} dR \quad (C-6)$$

then

$$A_{I_{\ell', \varepsilon', \ell \varepsilon}}^{\lambda} = \frac{1}{R_0} [I_{\lambda+1}^C(k_-, \theta_-, R_a) - I_{\lambda+1}^C(k_+, \theta_+, R_a)] \quad (C-7)$$

where

$$k_- = k' - k$$

$$\theta_- = \theta' - \theta$$

$$k_+ = k' + k$$

$$\theta_+ = \theta' + \theta$$

(C-8)

For $m = 1$ and arbitrary k and θ ,

$$I_1^C = -\cos(\theta) \text{Ci}(kR_a) + \sin(\theta) \text{si}(kR_a) \quad (\text{C-9})$$

$$I_1^S = -\cos(\theta) \text{si}(kR_a) - \sin(\theta) \text{Ci}(kR_a) \quad (\text{C-10})$$

where si and Ci are usual sine and cosine integrals defined in Abramowitz and Stegun²³ as

$$\text{Ci}(x) = - \int_x^\infty \frac{\cos(t)}{t} dt \quad (\text{C-11})$$

$$\text{si}(x) = - \int_x^\infty \frac{\sin(t)}{t} dt \quad (\text{C-12})$$

For $m > 1$, the integrals in Equation (B-5) and (B-6) may be evaluated by integrating by parts. For example, letting

$$Q_m^C = \frac{\cos(kR_a + \theta)}{R_a^m} \quad (\text{C-13})$$

$$Q_m^S = \frac{\sin(kR_a + \theta)}{R_a^m} \quad (\text{C-14})$$

the cosine integral in (B-5) becomes with successive integrations

$$\begin{aligned}
 I_m^C &= -\frac{Q_{m-1}^C}{(m-1)} - \frac{k}{(m-1)} I_{m-1}^S & (C-15) \\
 &= -\frac{Q_{m-1}^C}{(m-1)} + \frac{k}{(m-1)(m-2)} Q_{m-2}^S - \frac{k^2}{(m-1)(m-2)} I_{m-2}^C \\
 &= -\frac{Q_{m-1}^C}{(m-1)} + \frac{k}{(m-1)(m-2)} Q_{m-2}^S - \frac{k^2}{(m-1)(m-2)(m-3)} Q_{m-3}^C + \\
 &\quad \frac{k^3}{(m-1)(m-2)(m-3)} I_{m-3}^S \\
 &\quad \cdot \\
 &\quad \cdot \\
 &\quad \cdot
 \end{aligned}$$

or, more generally,

$$I_m^C = -A_1 Q_{m-1}^C + A_2 Q_{m-2}^S + A_3 Q_{m-3}^C - A_4 Q_{m-4}^S - A_5 Q_{m-5}^C + \dots \quad (C-16)$$

where

$$A_n = \frac{k^{n-1}}{(m-1)(m-2)(m-3)\dots(m-n)} \text{ for } n = 1, 2, 3, \dots, m-1 \quad (C-17)$$

By inspecting Equation (B-15) it is seen that the last term in the series for a given m is

$$(-1)^{m/2} k A_{m-1} I_1^S \text{ if } m \text{ is even, and}$$

$$(-1)^{\frac{m-1}{2}} k A_{m-1} I_1^C \text{ if } m \text{ is odd.}$$

Therefore, letting

$$S_N^C(m) = \sum_{n=0}^N (-1)^{n+1} A_{2n+1} Q_{m-(2n+1)}^C \quad (\text{B-18})$$

and

$$S_N^S(m) = \sum_{n=1}^N (-1)^{n+1} A_{2n} Q_{m-2n}^S \quad (\text{B-19})$$

we have for integer $q = 1, 2, \dots$

$$I_m^C = S_{q-1}^C + S_{q-1}^S + (-1)^q k A_{2q-1} I_1^S \quad \text{for } m = 2q \quad (\text{B-20})$$

$$I_m^C = S_{q-1}^C + S_q^S + (-1)^q k A_{2q} I_1^C \quad \text{for } m = 2q+1 \quad (\text{B-21})$$

Method 3: Approximate Radial Wavefunctions in the Centripetal Regime

In the absence of an isotropic intermolecular potential $V^0(R)$, the finite solutions to the Schrodinger equation are the spherical Bessel functions

$$j_\ell(\rho) = (2\pi/\rho)^{\frac{1}{2}} J_{\ell+1/2}(\rho) \quad \rho = kR \quad (\text{B-22})$$

which are proportional to ρ^ℓ for $\rho \rightarrow 0$ and have the asymptotic form

$$j_\ell(\rho) \rightarrow \frac{\sin(\rho - 1/2 \ell \pi)}{\rho} \quad (\text{B-23})$$

By comparing the asymptotic limits in Equations (B-2) and (B-23) it is seen that outside the interaction region the functions $\Psi_{\ell\epsilon}$ and j_ℓ differ only by the phase shift $\delta_\ell(k)$. In addition, since the shape of the wavefunction is determined mainly by the form of the potential to the right of the smallest classical turning point, the functions $\Psi_{\ell\epsilon}$ and j_ℓ are not very different when $k^2 < \ell(\ell+1)/\rho_R^2$ so that $\delta_\ell(k)$ is small when $\ell > k\rho_R$. Thus, in the centripetal regime (low ϵ , high ℓ),

$$\Psi_{\ell\epsilon}(R) \approx j_\ell(\rho) \quad (\text{B-24})$$

and

$$I_{\ell'\epsilon',\ell\epsilon}^\lambda \approx \frac{\pi}{2} (k'k)^{\frac{1}{2}} \int_0^\infty dR \frac{J_{\ell'+1/2}(k'R) J_{\ell+1/2}(kR)}{R^\lambda} \quad (\text{B-25})$$

This is a Weber-Schafheitlin type integral which for $\lambda > -1$ and $(\ell' + \ell - \lambda + 2) > 0$ is proportional to a hypergeometric function, i.e.,

$$I_{\ell'\epsilon',\ell\epsilon}^\lambda = \frac{Z^{\frac{C-1}{2}} k_{\max}^{\lambda-1}}{2^\lambda \Gamma(C) \Gamma(1-B)} {}_2F_1(A, B, C; Z) \quad (\text{B-26})$$

where Γ is the gamma function, ${}_2F_1$ is the Gauss hypergeometric series and

$$\begin{aligned} A &= \frac{1}{2} (\ell' + \ell - \lambda + 2) \\ B &= \frac{1}{2} (-\theta(\ell' - \ell) - \lambda + 1) \\ C &= A + B + \lambda \end{aligned} \tag{B-27}$$

$$Z = (k/k')^{2\theta}$$

with $\theta = \text{sign}(k' - k) = \pm 1$ depending on whether $k' - k$ is positive or negative and k_{\max} equals either k' or k depending upon which is larger.

$$\text{For } k' = k \text{ (} Z = 1 \text{),} \tag{B-28}$$

$${}_2F_1(A, B, C; 1) = \frac{\Gamma(C)\Gamma(C-A-B)}{\Gamma(C-A)\Gamma(C-B)}.$$

Since $C = A + B + \lambda$ with λ a positive integer, the hypergeometric function may be evaluated using Equation 15.3.11 in Abramowitz and Stegun¹⁵ for $k' \neq k$, giving

$$I_{\ell', \varepsilon', \ell \varepsilon}^{\lambda} = \frac{Z^{\frac{C-1}{2}} K_{\max}^{\lambda-1}}{2^{\lambda}} \frac{S_1 - S_2}{\Gamma(A+\lambda)\Gamma(B+\lambda)\Gamma(B)\Gamma(1-B)} \tag{B-29}$$

with

$$S_1 = \Gamma(\lambda)\Gamma(1-\lambda) \sum_{n=0}^{\lambda-1} \frac{\Gamma(A+n)\Gamma(B+n)}{n!\Gamma(1-\lambda+n)} (1-Z)^n \tag{B-30}$$

and

$$S_2 = (Z-1)^\lambda \sum_{n=0}^{\infty} \left[\frac{\Gamma(A+\lambda+n)\Gamma(B+\lambda+n)}{n! (n+\lambda)!} (1-Z)^n \times \right. \quad (B-31)$$

$$\left. \{ \ln(1-Z) - \psi(n+1) - \psi(n+\lambda+1) + \psi(A+\lambda+n) + \psi(B+\lambda+n) \} \right]$$

where ψ is the digamma function. In calculations the summation in Equation (B-31) is carried out until the relative difference between successive values for S_2 is less than a specified convergence tolerance.

Since λ is a positive integer, the parameters A, B, and C are integers divided by two. The parameters A and C are always positive and vary from 1 to $\ell_{\max} + 1$ and from $3/2$ to $\ell_{\max} + 3/2$ respectively, where ℓ_{\max} is the largest accessible value of ℓ . In addition, the selection rules on changes in the relative angular momentum, $-\lambda \leq \ell' - \ell \leq \lambda$, require that B varies from $\frac{1}{2} - \lambda$ to $\frac{1}{2}$.